# STUDY, DESIGN AND IMPLEMENTATION OF 3D PRINTER

HAMK
HÄMEEN AMMATTIKORKEAKOULU
HÄME UNIVERSITY OF APPLIED SCIENCES

Bachelor's thesis

Degree Programme in Electrical and Automation Engineering

Valkeakoski, Autumn 2019

Tung Nguyen

HÄMEEN AMMATTIKORKEAKOULU
HÄME UNIVERSITY OF APPLIED SCIENCES

Degree Programme in Electrical and Automation Engineering
Valkeakoski

**Author** Tung Nguyen **Year** 2019

**Subject** Study, Design and Implementation of 3D Printer

**Supervisor(s)** Juhani Henttonen

ABSTRACT

The trend of possessing individual 3D printers has been around for the last five years; high-performance printers, are however typically expensive and difficult to develop as well as to replicate. In addition, most of these commercial 3D printers feature single extrusion printing, the development of multi-material printing has not been extensively explored. The printer fabricated in this thesis was implemented to address these concerns.

To realize the target, fundamental concepts concerning mechanical designs, hardware components and controller were reviewed in addition to the possibility of multi-material extrusion. The discussed concepts were focused on the Fused Deposition Modelling (FDM) printing technology for 3D printers that are capable of replicating themselves.

All in all, the thesis presents a framework to construct a low-cost, multi-material 3D printer based on open-source design. In addition, users and operators are provided with a cross-platform interface for interacting and functioning the machine. The framework could be considered as a solution to self-replicating 3D printers, which students can adopt, fabricate for their own uses and engage deeper in engineering curricula. The open architecture of the printer allows independent and further development of the extension hardware and print heads in the future.

**Keywords** 3D printing, Additive Manufacturing, multi-material printing

**Pages** 41 pages including appendices 4 pages

Acknowledgement

Writing this thesis is an individual work; however, I would not be writing these words without relentless support from people whom I have met and worked with at HAMK, and in Valkeakoski.

I would like to express my greatest gratitude to Erkki Honkakoski, for inspiring, supporting and guiding me through my bachelor journey. Without you, there wouldn't be such an exciting and engaging project about 3D printers. To Ritva and Pekka Simula, thank you for trusting and caring me as a family member when I first came Finland and began the study here.

To Juhani Henttonen, I appreciate your approval to let me conduct this thesis work, and also your advice at early the implementation.

To mom, dad and little sister, I am blessed to have you in my life, for that I am forever grateful.

CONTENTS

LIST OF FIGURES

# 1 INTRODUCTION

Additive Manufacturing (AM) is an automated process for conversing computer-aid design (CAD) models into physical objects, by adding raw material layer by layer until the final shape is achieved. This process differs from most of traditional and long-established manufacturing processes that are subtractive in nature, where raw material is often being removed away from original block of material through carving, milling or machining. In terms of efficiency, as layer-wise manufacturing builds objects not by eliminating raw materials, the material waste is significantly reduced. In terms of flexibility, the layer-wise manufacturing approach allows manufactures to rapidly prototype designs and process multiple materials, without the need for extensive industrial infrastructure. For industries like aerospace and medical that heavily relies on lightweight and complex geometric parts produced in small volume, the cost savings of additive manufacturing offered are even more lucrative. Outside of the medical and aerospace industry domain, early adoption of additive manufacturing as way of product customisation has centred on consumer products such as toys, wearable devices, footwears and even executive cars (Reeves & Mendis, 2015).

The technology is well known for several decades in industry circles; however, the high cost of an AM machine has kept them beyond the reach of typical consumers. Until recent years, the use of AM, commonly known under the term “3D printers”, has become more widespread and more accessible to public uses. In particular, the introduction of inexpensive hardware, open-source design, and free license software 3D printers from the RepRap project allowed engineers and hobbyists to acquire an individual 3D printing machine at low cost. Its impact was such that the price of equipment has dropped whilst the diversity of models has increased and turned inspired to endless variety of desktop 3D printer designs (Lan, 2013).

In order to fully exploit the advantages of 3D printing, it is essential to understand the mechanism used in the machine, their limitations and their capabilities early during the design process. While there are many aspects evolving in the field of 3D printing, this thesis specially covers the fundamental of a Fused Deposition Modelling (FDM) 3D printer, including design considerations, material/component selection and implementation. To address these concerns, this thesis presents a framework of fabricating a 3D printer, which has the following design intents:

- Compact design: The printer is intended to accommodate all parts in an optimal volume, which entails that the actual printing volume is close as possible to the total machine volume.

- Low cost, high performance: The printer delivers a good balance between quality and cost, allowing students to replicate easily using low-level resources.
- Multi-material capability: The printer head is capable of dispensing multiple materials using a single extruder, enabling combination of physical properties in a single object.

Although affordable 3D printers have become popular among enthusiasts and hobbyists, yet there is comparatively little attention given towards the use of multi-material printing, focused on the consolidation of materials, material's interface quality, and how these compare to standard (single material) extrusion 3D printing. Most commercial 3D printers feature only a single extruder head to keep the machine cost down. Consequently, these printers are limited to either printing only objects that do not require any support material, or to not using the support material as reinforcement for other one. In addition to the core work of fabricating a 3D printer, the lack of information concerning multi-material 3D printing was, therefore, also the motivation for this thesis work.

The thesis is divided into seven chapters described as follows. Firstly, the theoretical basis of additive manufacturing and 3D printing are introduced in chapter two. Next, in chapter three, an overview of existing 3D printer designs today are reviewed, with an emphasis on addressing their advantages and shortcomings. Chapter four covers specific details of the printer's mechanical implementation. The control system and electronics implementation suited to the chosen hardware design is presented in chapter five. In chapter six, sample outputs produced, including multi-material structures, are analysed. Finally, chapter seven discusses current machine limits and possibilities to increase capabilities of the machine for future work.

# 2 BACKGROUND

## 2.1 Additive Manufacturing and 3D Printing

In the scope of manufacturing and industry, Additive Manufacturing is a term, referring to technique that grows three-dimensional objects by one layer of melted material at a time using a variety of approaches, whereas "3D Printing" specially associates with filament-based desktop printers among consumer-maker community. It is important to point out that AM does not constitute a single technology, in fact, it is a large umbrella term that many kinds of distinct technologies fit under, notably Stereolithography (SLA), Selective Laser Sintering (SLS), and Fused Deposition Modelling (FDM). The main different between these technologies are in the technique that layers are deposited to form parts and in the materials that are used.

Stereolithography (SLA) was the very first AM technology, where photopolymer resin is solidified selectively whenever ultraviolet (UV) light strikes, forming desired object layer by layer, as shown in Figure 1. The materials used in SLA are resins that come in liquid form and can be cured through exposure to UV light. These SLA printers are capable of creating parts with much finer resolution in a way that layers are nearly invisible to the human eyes – especially when compared to other printing methods such as FDM. However, produced plastics are UV-unstable and are unlikely to be suited to outdoor applications with extreme light exposure. In addition, the photo-curable resins, which are also hygroscopic; this means that they will absorb water, discolour and distort over time making them unsuitable for applications in appliances such as washing machines and dishwashers. For these reasons, SLA photopolymers objects are excellent for prototyping and master pattern applications at early stages of production, but their effect on the final production for permanent parts remains to be seen (Reeves & Mendis, 2015).

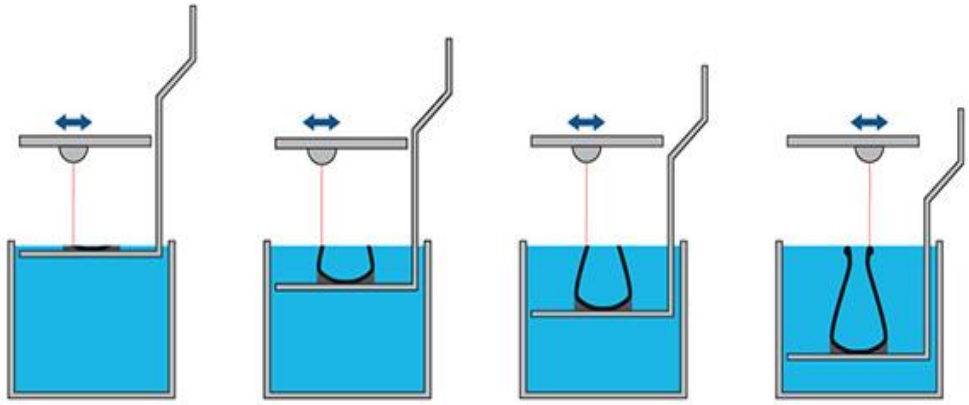

Figure 1. Cross view of the SLA process (Franky, 2014)

Selective Laser Sintering (SLS) is a similar technology that uses metal powder instead of plastic powder and, thus produces objects with required mechanical properties. In a SLS machine, a laser sinters metal powder layer by layer so that the metal particles are heated and fused into a solid connected pattern, as shown in Figure 2. Materials used in SLS cover a large range of metals and metal alloys, including aluminium, stainless steel, cobalt chrome and Inconel (Fabian, 2019).

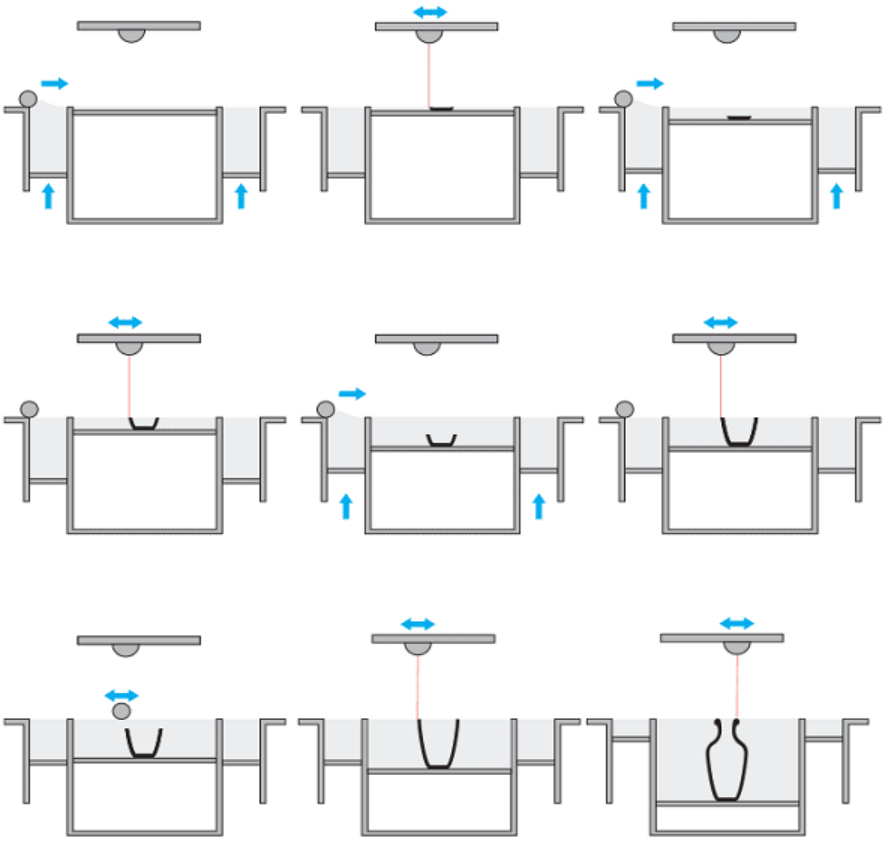

Figure 2. Cross view of the SLS process (Fabian, 2019)

In a Fused Deposition Modelling (FDM) machine, plastic in solid form is driven into a thermal head so called “nozzle”, which melts the material to liquid form and then deposits it onto a build surface in predetermined locations, as shown in Figure 3. Extruded layers of liquid plastic quickly fuse together as temperature cools, and another layer is bonded on top previously deposited ones to repeat the process until the three-dimensional object is built. The build size of a desktop FDM machine is typically 200 x 200 x200 mm and the dimensional accuracy is relatively low at 0.2 mm. In comparison, SLS or SLA may offer higher resolution print, but FDM is the most widely used 3D printing technology among the AM family due to the simplicity in mechanism and inexpensive materials involved (Varotsis, 2019).

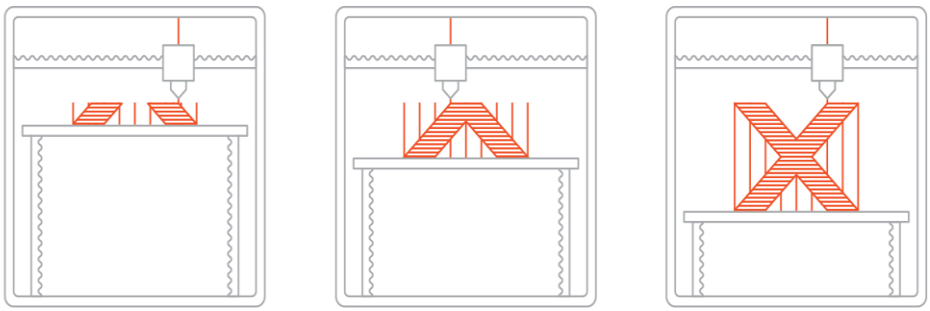

Figure 3. Cross view of the FDM process (Varotsis, 2019)

Fundamentally, all 3D printers have a same process for a digital model of the part to become a physical object. The process begins with a CAD modelling software to design a desired object and export the design in the STereoLithography file format (.stl). The first step could be also reserve engineering products with help of a 3D scanner or Photogrammetry. The model from an STL file is then processed by a software called “slicer”, which converts the geometric model into an array of thin layers and contains trajectory instructions to move the printer in a G-code file. The information in G-code file is essentially tailored to specific type of AM machine and precisely guides the machine where to deposit material on build surface. The next step is to transfer the G-code file to the AM machine and manipulate machine settings to achieve the optimal result. The machine setup parameters are important to balance the quality of the part and the speed of production. After object has been designed and preparation done, the printing process is executed entirely automatically, involving height calibration, material deposition, layer formation, until the final shape is achieved or no material remaining (Redwood, 2017).

Although manufactures had actively embraced this technology for decades, their high price had kept them to a small segment of manufacturing industry. It was not until 2010, the cost of 3D printing machines has decreased dramatically, a typical FDM machine that used to cost $30,000 now costing under $1000 while keeping the cores features and functionality fully in place. Such advances are possible thanks to the introduction of low-cost hardware, open-source design, and free software licensed 3D printers initiated by a community project called “RepRap” in 2005. In particular, the RepRap project features versions of “desktop” 3D printers built on 3D printed parts. To bring the price down, these desktop 3D printers are made from inexpensive structural components such as acrylic, plywood, or aluminium. When the FDM patent fell to the public domain in 2009, the open-source nature of RepRap project has enabled users to replicate and modify the printer’s mechanical design and firmware code. Community of makers and engineers were now free to design

products and create prototype on their own 3D printers rather than relying on companies or technologies firms. Consequently, several variations of modifications to extend machine capabilities have been contributed online for other users to reproduce (RepRap, 2016).

## 2.2 **Multi-material Printing**

In traditional manufacturing, when designers attempted a combination of colours or physical properties in a single object, they would express the object out of the combination of smaller parts, each part having the desired properties. Hence, achieving the combination of engineering properties is still a complex practice, either complicating the design process, or complicating the manufacturing process. As additive manufacturing works by only depositing materials where it is instructed, it opens the possibility that objects can be composed of several materials, each differs from one another in terms of aesthetics or physical properties (Lan, 2013).

Unfortunately, most 3D printing techniques in AM are unable to satisfy this goal. In the SLA process, the limitation would appear obvious in the machine setup: it requires a tank of liquid resin functioning as build material and build surface, and the build material cannot be changed without draining the rest of current build material out of the tank; which is a time-consuming and impractical procedure. Mixing two different kinds of resin together in a tank could be an alternative; however, the results would be unpredictable and achieving a right proportion for the mixture on the fly is again an impractical implementation. In the sintering process, there are clear physical limitations in co-sintering two materials with different melting or sintering temperature (Bandyopadhyay, 2019).

A 3D printer using FDM technique is better suited to processing material changes within layers. Most commercial 3D printers did in fact approach using multiple extruders to allow switching between materials; however, the primary drawbacks of these printers are the reduction of the available build volume and the calibration of extrusion heads. The former issue is a direct consequence of accommodating the additional extruder(s), commonly placed side-by-side in a direct drive system. The reduction of the available space is proportional to the distance between extrusion nozzles, the dimensions of the extruders, and the number of the extruders attached. Without changing the machine frame, this limitation is impossible to overcome, thus, resulting to a higher up-front cost to manufacture a larger build volume. The latter issue with multi-extruder setup is the need to ensure/maintain a precise alignment of the two, or more, extrusion hotend(s) during the printing process. This a time-consuming procedure that involves some trial-and-error cycles of positioning, printing and assessment to assure an adequate macroscopic

continuity of printed object whenever an active extruder has switched (Lopes, Silva, & Carneiro, 2018).

Given the current shortcomings in the field of 3D printing, the thesis work presents a multi-material printing solution using the two-to-one Bowden extrusion, where several materials are routed into a single print head. In this setup, the extruder, which guides each material, is detached from the moving print head and the build space of the machine. In order to allow switching between different materials, the current printing material is retracted far enough from the print head, so that the other material can take the same path and come in. As the extruders are located outside of the printing volume, the issues with calibrating positions, consumed space by additional hotend(s) are eliminated while attaining similar results.

# 3 DESIGN PROCESS

The 3D printing process is achieved by positioning an extrusion head in three dimensions relative to the build surface: two dimensions are required to produce a single slice, and one more is required to reposition the system to create additional slices on top of previous ones. Accomplishing three degrees of positioning movement requires at least three degrees of actuation. Theoretically, this positioning mechanism may be carried out via several approaches, such as revolute robotic arms or combination of linear axes. The question lies on how to efficiently distribute actuation in three directions of X/Y/Z between the print head and the build surface. In general, designs of 3D printer can be separated into four categories based on their mechanical arrangement: Delta, Cartesian, SCARA and Polar; each with their specialized application. Since neither SCARA nor Polar are yet mature and well supported by open-source software, they will not be discussed in the scope of this thesis. In any case, the design process for a 3D printer is outlined by a selection process of three independent subsystems (Lan, 2013):

- Linear motion system
- Feed mechanism
- Mechanical frame

## 3.1 Mechanical Arrangements

Since the printer's motion system must be able to position the print head in a three-dimensional space, the first approach of 3D printer design was straightforward to arrange three perpendicular axes per each linear X-, Y-, and Z-direction, known as Cartesian coordinate system. This standard design is often used in CNC milling, routers and variety of 3D printers in both industrial and desktop. A typical "Cartesian-XZ-head" design uses X-axis to move the print head; the Z-axis in turn moves the entire X-axis,

providing the second degree of freedom, as shown in Figure 4. This configuration is perhaps the most replicated version of desktop 3D printer (RepRap, 2014) thanks to the ease of understanding kinematics, where each of the motors only actuates one direction. The main advantages of Cartesian-XZ-head printer are simplicity and high degree of isolation between axes. On the other hand, the biggest drawback of this design is that the load for each axis is different, as X- and Y- only carry the mass of the carriage and the build platform, whereas the Z-axis must move the mass of the carriage, the X-axis, and their motors. Consequently, there are some issues with the thickness of the object, known as Z-wobble, as the printing becomes very tall.

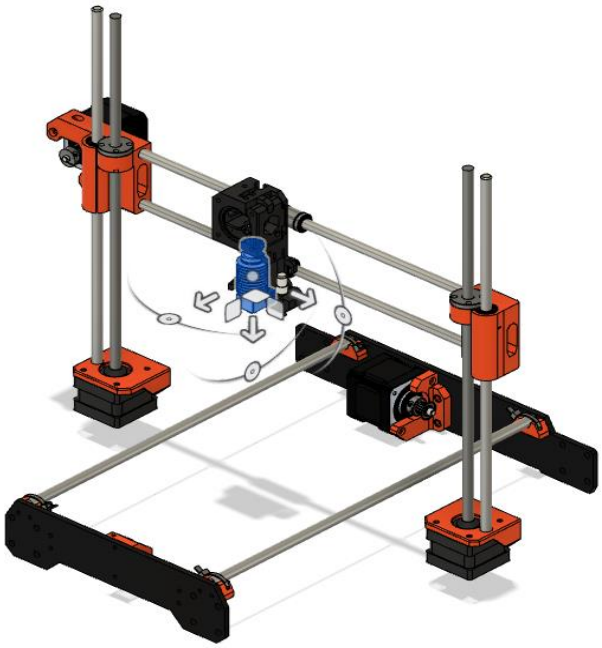

Figure 4. Cartesian-XZ-head design (Swesen, 2018)

One variant of Cartesian mechanism is the “CoreXY” design, as seen in Figure 4. The mechanism working by lifting/lowering the build platform only in Z direction and using two stationary motors to drive the print head in both X and Y directions, allows the print head to move simultaneously in XY plane. As illustrated in Figure 5, in the CoreXY mechanism rotating both motors in the same direction results in horizontal motion. Conversely, rotating in the opposite direction results in vertical motion. A CoreXY printer is an example of parallel manipulator system that uses chains of actuators to support a single end-effector. Parallel manipulator systems have an advantage of much lower inertia than the serial stack-up arrangements, such as Cartesian-XZ-head mentioned above (where their motors must carry the mass of other motors). The lower inertia of a parallel manipulator, with the same given torque and same actuators, permits more rapid accelerations and faster movements than the serial stack-up arrangements (RepRap, 2015).

One potential drawback with the CoreXY design is that when the carriage moves at 45° and 135°, only one motor is moving and must supply all torque required to move the entire mass of X- and Y- axes. If the printing layer is shifted from predetermined coordinates, it often occurs when printing infill at diagonal lines of 45° or 135°. Consequently, the control schemes for the two motors must be able to compensate the speed, acceleration, and junction deviation (or jerk) to low values in such cases. Another disadvantage of the CoreXY setup is long belts and multiple pulleys used. The accuracy of positioning relies on the stiffness of the belt; however, belts tend to stretch and act like springs, when pulleys are out-of-square under high angular stresses. The ringing/vibration generated by belts may cause harmonic resonance at certain printing speeds and distort the printed parts.

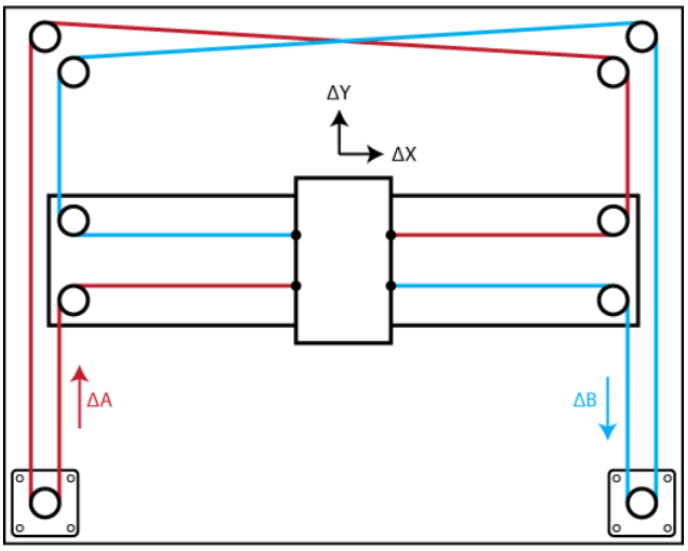


Figure 5. CoreXY design (CoreXY theory, 2012)

Another candidate of the parallel manipulator system is the Delta Bot configuration that uses three rigid arm pairs controlled by three identical actuators to achieve positioning in three dimensions, as illustrated in Figure 6. Three pairs of arms are set in an equilateral triangle and transfer motion to a single end-effector mounted between the tips of these arms. There are many solutions existed to manipulate arm pairs, but only two are used in common practice (Delta geometry, 2016):

- Rotational Delta: Each arm pair is connected to a main articulated arm, or an elbow joint, and this main arm is actuated directly by a servomotor attached on the top of the frame. This solution is widely used in automated process such as 'pick and place' of a production line due to the setting can be mounted directly to the frame above the workspace.
- Linear Delta: Each arm pair is attached to a carriage sliding on a linear rail, which slides along the three columns in the frame. Each carriage's position is controlled by a stepper motor mounted at the

bottom of the frame. This solution is the most frequent type used in 3D printing industry, due to the ability to move more mass than the rotational Delta.

The kinematic calculation of a linear delta system is based on the relationship between the positions of the three carriages and the location of the end-effector. As the carriage only moves in a straight line, so the change in horizontal movement of the end-effector is linked to the change in vertical movement of the carriage by Pythagorean theorem (which states that, in a right triangle, the hypotenuse length squared, is equal to sum of other two sides squared).

As depicted in Figure 6, the hypotenuse in this case is the arm length; the vertical edge is the relative vertical position of the end-effector and the carriage; the horizontal edge is the relative horizontal position of the end-effector and the carriage. Control of a linear Delta design is difficult, if not impossible, as the control scheme constantly receives the end-effector positions in Cartesian coordinate prescribed by the G-code as input and must turn it into actuator positions through a mathematical model, known as inverse kinematics (Graves, 2015).

The biggest advantage that Delta printers offers 3D printing industry, undoubtedly, is that they have the potential to print very quickly, and speed is one of the key factors to assess performance of 3D printers. In addition, as the build platform and motors remain stationary in the frame, the system has a minimum moving mass, and this eliminates a major source of complexity and potential problems.

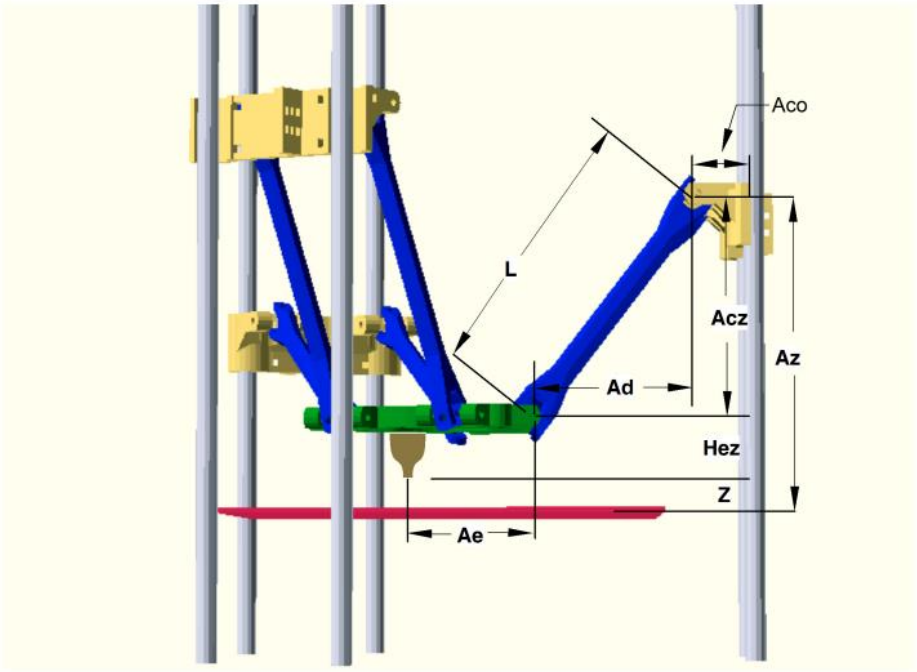


Figure 6. Linear Delta design (Graves, 2015)

## 3.2 **Linear Motion System**

Regardless of the mechanical arrangement used in 3D printer design, the linear motion system is considered as the most crucial mechanism in providing the axial movement with high precision. The linear motion axis must be stiff enough to prevent backlash and unwanted deflection, while allowing fast and stable motion in desired direction. These criteria are accomplished by selecting three physical components with care: an actuator to produce motion, a transmission to transfer motion and a linear guide to constrain motion (Lan, 2013).

### 3.2.1 Linear guides

The linear guide consists of a moving carriage that slides back and forth along a linear element called a rail, and it comes in two basic shapes – round and square. As the carriage initially has six degrees of freedom, three rotational degrees of freedom and three translational degrees of freedom, the linear guide must eliminate five degrees of freedom to produce desired motion (Rosenberge, 2018).

Traditional designs for CNC machines, shuttle devices and working holding devices uses dovetail slides as linear guides, as shown in Figure 7. A dovetail slide is flat on top and bottom, while the side has a concave shape, or dovetail-shaped which locks the carriage into the base. They are ideal selections such as machine tools that require high load capacity and high accuracy positioning. However, dovetails slides have difficulties with high friction, and it makes them poor choices for short traverses in 3D printing. Additionally, as the dovetail slides have such a large contact area, the carriage requires careful manufacturing of the mating surfaces from cast iron, hard-coat aluminium or stainless steel, raising the cost significantly (Collins, Linear Motion Tips, 2017).

Figure 7. Dove-tail slide (Collins D. , 2018)

Another alternative to a linear guide is using linear ball bearings riding on a smooth shaft. Inside a linear ball bearing, there are two linear rows

contained of tiny recirculating balls made of metal, which support the carriage for smooth linear movement along the shaft. Ball bearing slides offer low-friction motion and hence require less force to move than a design using dovetail slides. However, ball bearings have a lower load capacity for their size, and they allow free rotation of the carriage around the shaft. To mitigate this limitation, some 3D printer designs utilize a pair of shafts to fully constrain the carriage, as shown in Figure 9. In addition, because dirt and dust can accumulate in the lubricant (usually grease), the tiny balls eventually run louder and scratch surfaces of the shaft. Therefore, linear ball bearings require a regular interval of maintenance to retain performance.

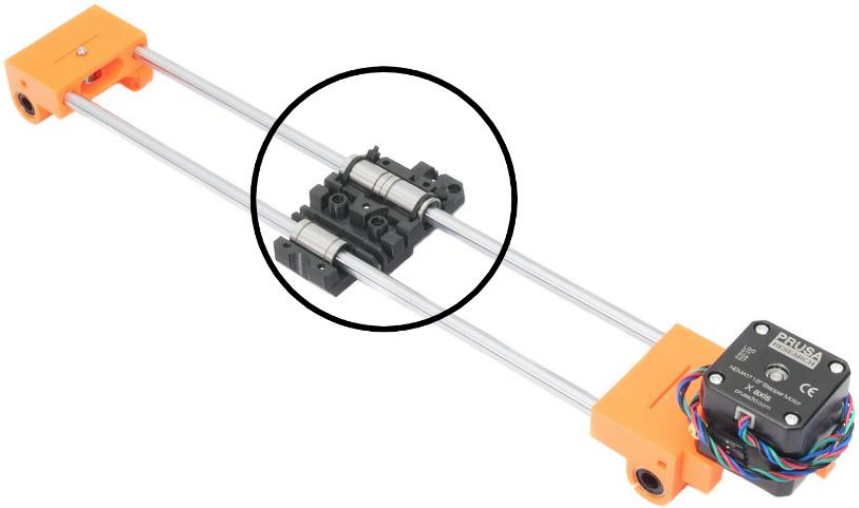

Figure 8. Linear ball bearings and guide shafts (Dolezal, n.d.)

A related design replaces the linear ball bearings with the polymer bushings, which rely on two smooth surfaces riding on one another, as shown in Figure 9. High-end polymer bushings are self-lubricating by depositing a tiny amount of lubricant that is an integral part of the polymer blend. Hence, they are low friction and long-wearing than a design using linear ball bearings. However, the part consuming itself in order to function means that it will degrade after a number of cycles.

Figure 9. Polymer bushings (drylin® linear guides, 2019)

Another design of linear guide, one that has been adopted widely in the low-cost 3D printer in recent years, is the wheel-type linear guide, as shown in Figure 10. This design uses two or more wheels riding along an aluminium rail, and each wheel is fully engaged in the mating slot(s) in the aluminium rails, thus providing well controlled, low-friction rolling contact.

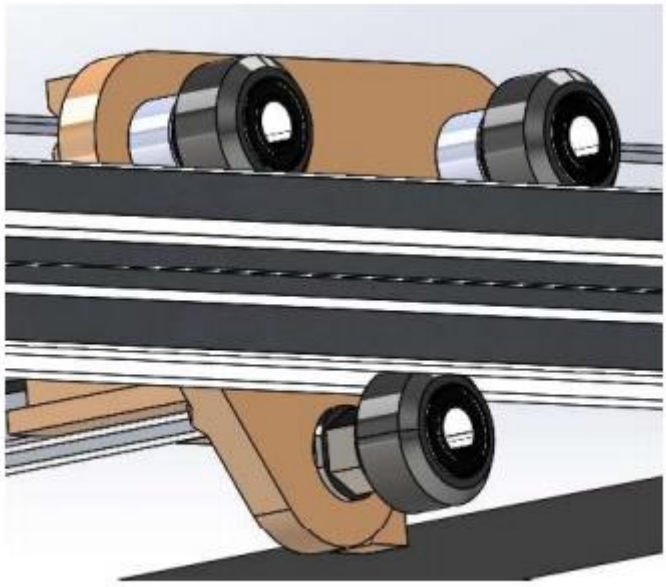

Figure 10. Wheel-drive linear guide (Rosenberge, 2018)

### 3.2.2 Transmission

The transmission is responsible for transferring motion between actuators and the carriage. Unlike pneumatic or hydraulic actuators that naturally produce the linear motion, the transmission using electric-powered actuators must also be able to convert the rotary motion into desired linear motion.

The first concept to explore is a linear system using lead screw, pictured in Figure 11. A lead screw system consists of a screw, which is rotated by the motor, and a mating nut that moves bidirectionally along the length of the screw as it rotates. This mechanism converts the relative rotary motion between a screw and a mating nut to a linear motion. Lead screw has many mechanical advantages. Firstly, it has high forces density, meaning that the system is capable of positioning heavy loads. Secondly, the lead screw system is non-backdrivable if the lead angle is low enough, and the vertical load will not cause the screw to turn. The elimination of backlash allows lead screw to easily self-lock for vertical application, as the drive motor

does not need to exert a holding torque to maintain the carriage's vertical positions (Santons, James, Chris, & Maalouf, 2015).

The downside of using lead screws is that systems cannot move quickly, and the maximum travel speed is limited, as they generate heat significantly due to sliding friction between the screw and the nut. High energy loss due to friction means that a greater torque is demanded by the drive system, lowering its efficiency. If the system experiences significant heat fluctuations, the expansion of mechanical components due to thermal effects can degrade a system's repeatability and accuracy. For these reasons, lead screws are not ideal choices for frequent motion along in X- and Y- directions of 3D printer but provide exactly required features for slow movement speed such as lifting/lowering the build platform along the Z-axis.

Figure 11. ACME lead screw (Toglefritz, 2015)

In order to reduce the friction seen in lead screws, most modern machine tools utilize ball screws, which replace the mating nut with a ball bearing that acts as precision unit, as shown in Figure 12. Ball screw inherits most advantages of lead screw, including supporting heavy loads and providing accurate positioning, but are more efficient thanks to the absence of sliding friction. However, ball screws are more complicated to manufacture and hence are more expensive than lead screws (Lan, 2013).

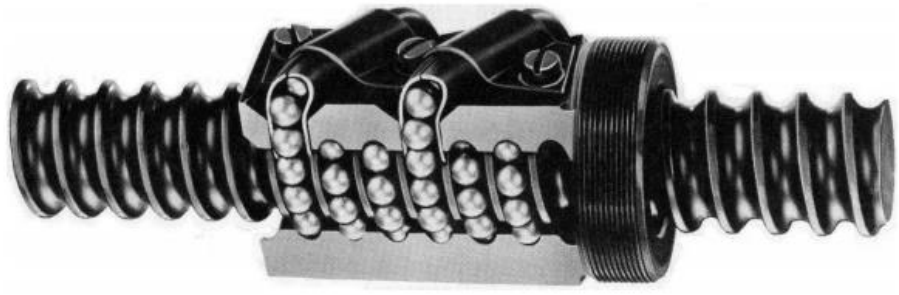

Figure 12. Ball screw (Toglefritz, 2015)

In order to provide more rapid movements than lead screw or ball screw systems, belt-driven systems are used on most 3D printers, as illustrated

in Figure 13. Ordinary belts, such as v-belts in cars, are not required to act as precision unit, and thus have a smooth surface. On the contrary, in 3D printers it is imperative to synchronize the rotation of the stepper motor precisely and permanently with the desired motion. For this purpose, the belt-driven system in 3D printer utilizes a special version of belt called "timing belt". A belt-driven system converts rotary motion to linear motion via a timing belt connected between two circular pulleys. The timing belt contains teeth that interface with the teeth on the pulleys to transfer torque and avoid slipping. Due to their low mass, belt-driven systems are preferred for applications requiring long travel distances and high speeds (Lan, 2013). Another benefit of using timing belt with carefully designed tooth profiles is that systems can have little to no backlash.

The main weakness of a belt-driven system is that belt is elastic. As timing belts tend to stretch over time, belt drives are less accurate than screw drives and can generate some vibrations to the system. For this reason, belt-driven systems usually incorporate some tensioning/re-tensioning mechanisms to ensure an adequate tension of the belt and prevent the system from lowering performance.

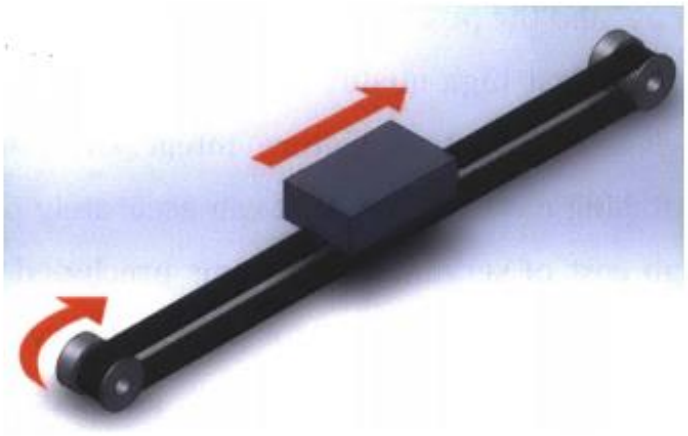

Figure 13. Belt-driven system (Lan, 2013)

### 3.2.3 Actuators

The final component of a linear motion for 3D printers is the actuator, precisely the electric-powered motor. Typically, choosing an appropriate actuator require knowledge mechanical requirements: mechanical load, accuracy, velocity, etc. In the context of 3D printers, there are three primary types of actuators: servomotor, DC motor and stepper motor (Lan, 2013).

Most high-quality motion control systems use servomotors for positioning. These high-torque motors comprise integrated rotary encoders to provide feedback for a closed loop system and are used with matching drivers to

accurately rotate the motor's shaft to any angle. In general, servomotors are excellent at delivering a consistent torque across the speed range of the motor and an accurate positioning, as a result of closed-loop operation. These benefits are undeniably helpful in traditional manufacturing technologies where the required torque is critical but are not particularly relevant in applications requiring low torque such as 3D printers. Since the dynamic forces in a 3D printer are nowhere near as strong as they are in CNC routers, milling machines, etc. Moreover, the cost of a servomotor system can be easily several times the price of an ordinary DC or stepper motor system, whereas the reliability of the positioning system increases slightly. The opportunity to improve system's reliability should be those likely on the rigidity and the orientation of belt, pulleys, linear guide, frame, etc., at first place (Rosenberge, 2018).

On the other hand, stepper motors give reliability at a lower cost and offer a more robust system with less electromechanical parts. The output movement of a stepper motor is subdivided into a number of fixed "steps"; when the stepper controller receives an input signal, the motor's output shaft will rotate over a fixed angle and then stop and hold that position. The above-mentioned feature makes it possible to control a stepper motor in an open-loop operation without the need for feedback sensors. However, typical stepper motors are 1.8 degrees per step or 200 steps per revolution, which is insufficient for more precise positioning applications. Hence, an extension to improve positioning resolution is to use a microstepping driver, which subdivides each full step of the motor into smaller steps. For example, a 1.8-degree step now can be divided up to 256 times, providing a step angle of 0.007 degrees or 51,200 steps per revolution. Microstepping is considered a good alternative to mechanical gear reduction in low torque applications because it does not introduce backlash into the system or reduce the system's maximum speed (Collins, Linear Motion Tips, 2017). The primary downfall of using stepper motors in open-loop operation is positioning slip: if an excessive load is applied to the output of a stepper motor, the motor's shaft may stop rotating, causing the motor to "miss steps", and the positioning system to lose synchronism with the input signal (Lan, 2013).

An alternative option to compromise above issues would be to use a traditional DC motor to actuate the axis, equipped with an encoder to keep track position – in essence, a low-cost scratch-built version of servomotor. It is possible to embrace the feedback mechanism with either a rotary encoder, or a linear encoder. In the former approach, as the encoder must be mounted on the motor's shaft, there is no actual position control of the carriage registered, because only the position of the motor's shaft is being controlled. To be able to verify the carriage position, the drive system must have a known and repeatable behaviour. On the other hand, the latter approach is more preferred as it gives a direct indication of carriage's position. Though the combination of using these high-torque motors coupled with encoders offers the system balanced dynamics, it also raises

concerns about machine safety. If an encoder failed during the operation, there is no longer an accurate indication of encoder position and producing torque. In many situations, this failure would result in a catastrophic event since the motors usually attempt to correct the error by giving more power.

For this thesis work, stepper motors were used to deliver the best reliability and safety for their cost. The possibility of missing steps caused by excessive loads is the primary weakness of a stepper motor, but this weakness can be partly mitigated with the recent advancement in developing microstepping drivers in recent years, especially with the stallGuard feature introduced in trinamic ICs. In order to detect loads on the motor, stallGuard measures electrical energy flowing into the motor and the energy flowing out of the motor again. The gap between both energies provides an indication of mechanical load taken from the motor. Furthermore, stallGuard measures which part of the energy fed to the motors goes back to the power supply. This spare energy is a measure for the mechanical load applied on the motor. If no spare energy remains and the motor may stall, the control system can response in time by pausing the motion and waiting for user's next actions to ensure the safety at an appropriately level (TRINAMIC, 2016)

## 3.3 **Feed mechanism**

In a nutshell, the feed mechanism refers to the delivery of the filament between the extruder and the print head to form printed parts, pictured in Figure 14. The extruder is the upper part that physically drives the solid filament forward and often comprises of a feeding gear, bearing and a stepper motor. On the contrary, the print head is where the filament is first melted to liquid form and then comes out the nozzle to become part of the 3D-printed object. There are two extrusion mechanism to drive the filament in desktop 3D printers: Direct drive and Bowden drive mechanism (Rosenberge, 2018).

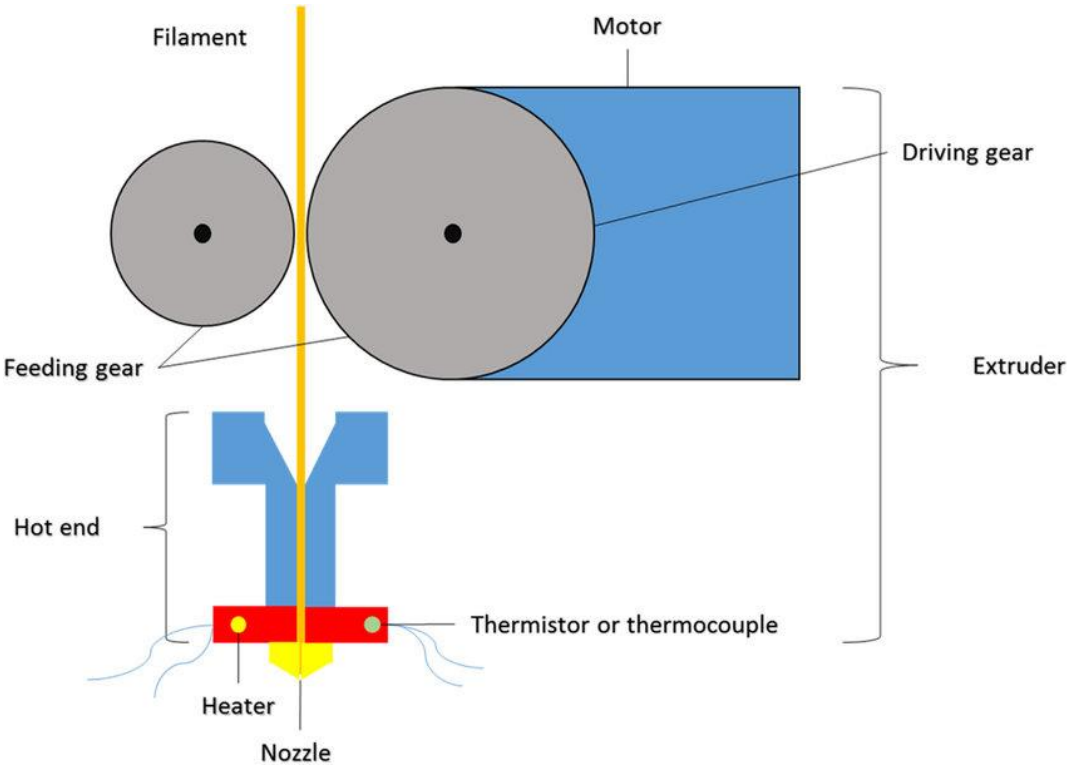


Figure 14. Feed mechanism (Zhang, Patil, Feng, & Tiwari, 2016)

In the setup of a Direct drive mechanism, the feeding gears are mounted on top of the print head and the filament is driven straightforward down through the extruder and into the print head, as shown in Figure 15. As a direct-drive mechanism keeps the distance that filament travels from cold end to hot end to a minimum, it gives better responsiveness to extrusion and retraction. The better responsiveness can create more stable material deposition, which in turn translates to less stringing, oozing, and other distortions on the printing surface. Given a shorter travel distance, the extrusion requires less torque from the stepper motor to drive the filament, and a lower torque means the feed mechanism can use the same size of motor at a lower current draw than in the equivalent Bowden drive. However, as the whole Direct Drive system is attached directly to the hot end, moving weight is added to the carriage. This extra mass can introduce more backlash and overshoot when printing at higher speeds. Adding a second extruder to allow multi-material printing is not a feasible option in Direct Drive systems, as the increased moving mass of the carriage is twice as much as a single extruder (Landry, 2016).

In the setup of a Bowden drive mechanism, the feeding gears are detached from the moving carriage and mounted to the static frame of the printer, as shown in Figure 15. The filament is driven to the moving head through a low-friction Teflon tube and enters the hot end. Bowden drive systems are well known for their ability to print at faster speeds, in comparison to Direct Drive systems, due to their lower moving mass. In addition, the separation of the extruder gears from the hot end assemblies enables a

Bowden system to embrace additional extruder gears onto the fixed frame of the 3D printer. This in an important feature to open possibilities of multi-material printing in 3D printers. A major disadvantage of a Bowden drive system is that the elastic filament tends to compress over the long length between the gears and the nozzle, which makes it more difficult to ensure a uniform flow rate of the filament. The filament also experiences increased friction in the Teflon tube, and more friction leads to a slower response time in the extrusion system (Landry, 2016).

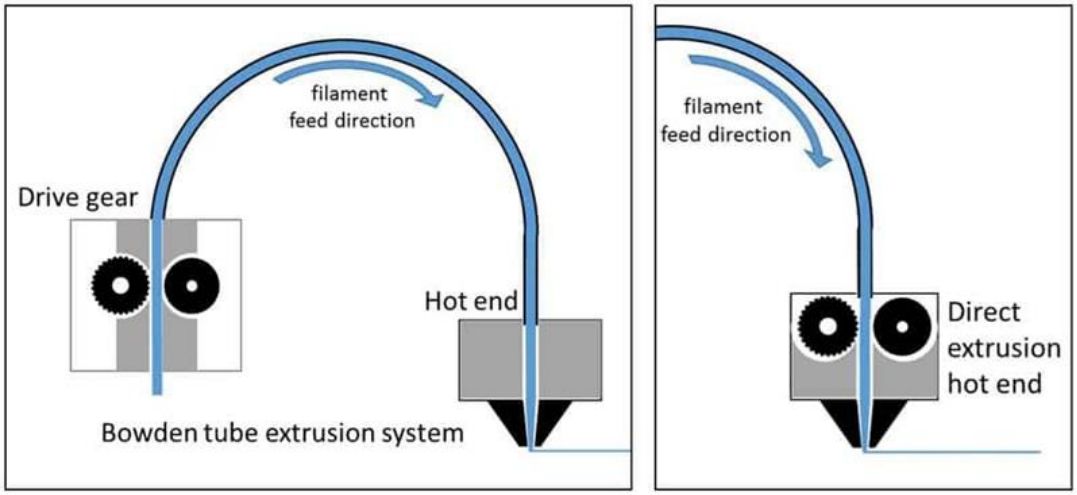


Figure 15. Bowden drive (left) and Direct drive (right) (3D Printer Power, 2018)

## 3.4 **Mechanical frame**

When the linear motion system and the feed mechanism are known in the design of 3D printer, the frame material and structure are designed based on the previous subsystem decisions. The frame often comprises a combination of metal and plastic parts to accommodate major components such as linear slides, the build platform, electrical components, the extruder, etc. Besides, as most 3D printer mechanisms rely on linear motion in order to move the carriage, the accurate alignment of a mechanical frame is essential to ensure that the linear guides position properly (Santons, James, Chris, & Maalouf, 2015).

A member construction with aluminium beams/extrusions is perhaps the most frequent choice for supporting the requisite structural strength in CNC machinery, 3D printers, furniture, structural hardware, vehicles and much more. These aluminium extrusions are lightweight, easily manufactured and can be connected by joints easily. When it comes to assembling structural frame using basic tools, instead of welding and complex joining, aluminium extrusions are more beneficial than solid counterparts such as steel (Santons, James, Chris, & Maalouf, 2015). There

are many different shapes of extrusion aluminium available. The shape of the cross section is called “profile” and two main profiles are used: T-slot and V-slot. The T-slot profile, also known as 80/20 profile after its creator 80/20 Inc., consist of extruded aluminium with a T-shaped groove on each side as shown in Figure 15.

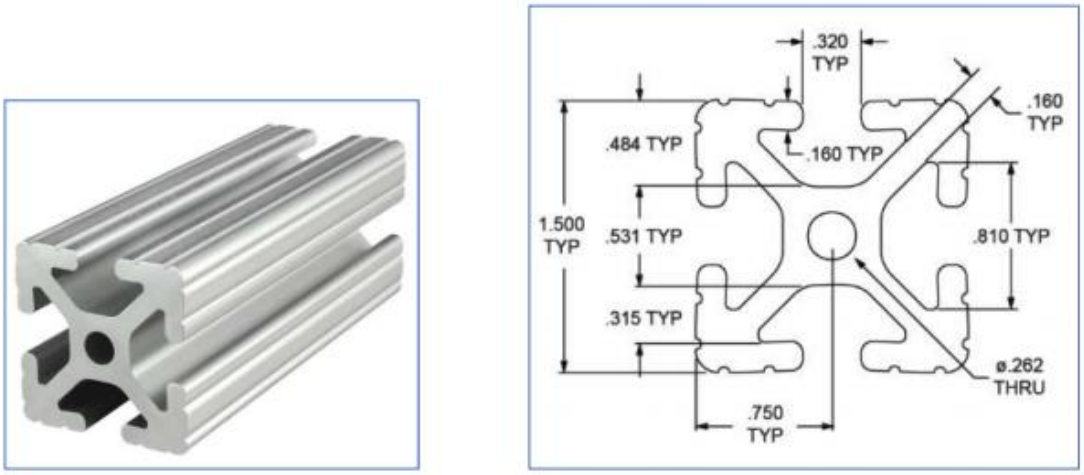


Figure 16. T-slot aluminium extrusion (Rosenberge, 2018)

The V-slot aluminium profile is a descendant of the above-mentioned 80/20 profile but has the distinction of having a V-shaped groove on four faces, as shown in Figure 17. Though this adjustment may seem like a minor difference, it brings a big impact to its usage. V-slot allows V-shaped wheels can ride on smoothly, meaning that it can be double used as linear rail and as structural frame, reducing the cost of parts for the linear motion system. In addition to V-grooves, a small 4.2 diameter circular hole is integrated in the middle of extrusion. The hole may be readily tapped with either an M5 or 10-32 screw, allows mounting parts to the end of the rail (Rosenberge, 2018).

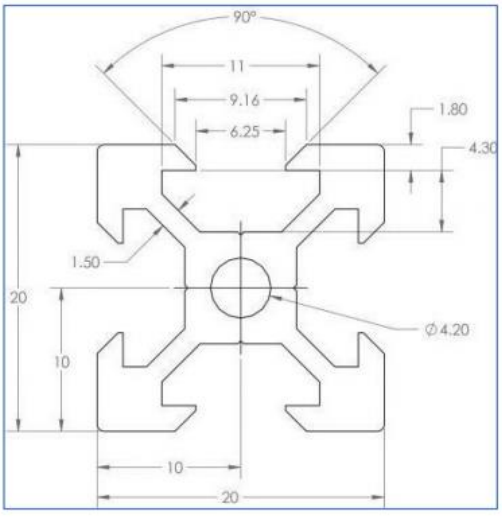


Figure 17. Cross section view of V-slot extrusion (Rosenberge, 2018)

A laser cut/CNC machined frame is another option for framing a 3D printer out of inexpensive materials such as plywood and acrylic, as shown in Figure 18. As wood and acrylic are light, relatively strong and easy to work on, they are one of the best materials for quick prototyping, medium sized robots and as construction aid. Materials are laser cut or CNC cut into puzzle-piece panels in a way so that they can be bolted together to form the final frame structure. It is no doubt that the low-cost construction and the ease of implementation of these frames are appealing benefits; however, they are fragile and more prone to obsolescence than the metal counterparts. Neither acrylic nor plywood are well resistant to the thermal effect for long terms. Moreover, woods warp easily as humidity changes. Hence, 3D printers built on wood/acrylic frame are limited to either printing without the heated bed, or to printing only materials with low heating requirements (RepRap, 2010).

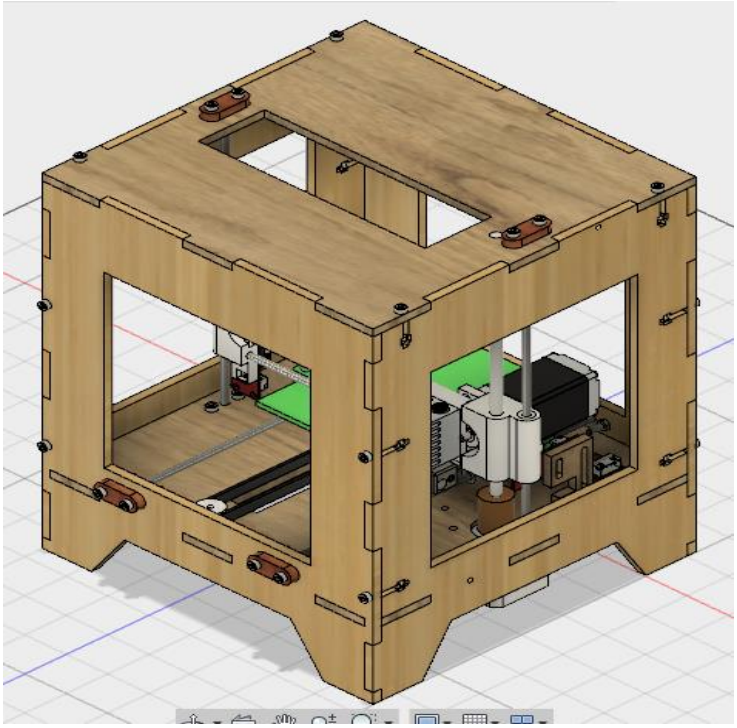

Figure 18. 3D printer with wooden frame (mmar896, 2016).

## 3.5 **Final design**

For this thesis project, the open source “Prusa i3” 3D printer design was chosen to be studied and implemented, as depicted in Figure 20. The decision to adopt the Prusa i3 design was made because of two primary reasons. First, since a traditional Cartesian arrangement is compartmentalized, the three X-, Y- and Z-axis can be developed and assembled independently. On the contrary, the mutual stiffening nature of parallel designs means that their design, implementation and calibration is more complex. Once the printer is fully built, in the traditional design the calibration process for each direction can be carried out sequentially

rather than having to calibrate multiple axes simultaneously. Calibration process refers to the work of verifying that all individual components should work as intended and applying adjustments when necessary. Errors and misalignments are inevitable, and at the end user should be able to calibrate/recalibrate the printer, so the ease of calibration is an important factor to improve the reliability of system. Secondly, as the printer is intended to embrace the extension of multi-material printing, a simple yet functional mechanical design is needed, whereas balanced dynamics are less critical than they might be.


Figure 19. Design of Prusa i3 3D printer (Swesen, 2018)

# 4 MECHANICAL IMPLEMENTATION

In general, the chosen design features stepper motors as the actuators for all three axes of the printer. As mentioned earlier, stepper motors are the most cost-effective option, and are capable delivering desired functional requirements. Each stepper motor has 200 steps per revolution and is

coupled with a TMC5160 stepper driver operated at 1/16$^{th}$ microstepping mode to provide an acceptable positioning resolution.

## 4.1 Implementation of X-axis

The printer achieves X-axis motion by driving a timing belt/pulley system with a pair of smooth rods, as shown in Figure 20. Pulleys and belts are used to convert the rotary motion of the motor to linear travel of the carriage, and two parallel rods are necessary to constrain the motion to a straight-line movement. The carriage that carries the print head is fully 3D printed and slides along the smooth rods on four polymer bushings. The utilisation of bushings can avoid regular maintenance with lubricant in future as bushings run dry, hence they do not have a propensity for attracting and accumulating dirt. There are two important points when constructing a timing belt/pulley system; ensure that the belt is taut, but not excessively, and support the idlers and pulleys well so that belt tension will not pull them off-angle (Rosenberge, 2018).

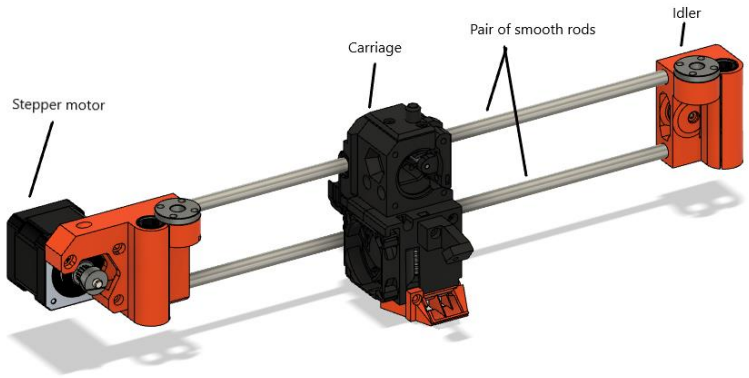


Figure 20. Design of X-axis (Swesen, 2018)

When transferring motion from a motor to a carriage, it is essential to determine how far the carriage will move with respect to motor rotations. The equation is basically straightforward – count the number of teeth on the pulley and multiply it by the pitch of the belt (Rosenberge, 2018):

$$D_{rev} = p \times N_t \ (1)$$

Where:

- $D_{rev}$ is the distance of travel per revolution, in millimetres;
- $p$ is the pitch of the belt, in millimetres;
- $N_t$ is the number of teeth on the pulley

As the pulley used on X-axis has 20 teeth and the timing belt used is a standard GT2-2mm pitch type, the travel distance per revolution is calculated as follows:

$$D_{rev} = 20 \times 2 = 40 \text{ (mm)}$$

Additionally, since the stepper motor receives input signals as a number of "steps" to rotate the motor's shaft to a certain angle, the control scheme must know how many steps the motor will take to move the respective carriage one millimetre:

$$E_{steps/mm} = \frac{E_{rev} \times f_m}{D_{rev}} \quad (2)$$

Where:

- $E_{steps/mm}$ is the number of steps required to move the carriage one millimetre;
- $E_{rev}$ is the number of total steps per motor revolution
- $f_m$ is the microstepping factor of the driver, e.g. 4, 16, 32;

As the motor used for actuation owns a resolution of 200 steps per revolution, and the microstepping driver divides each step into 16 smaller steps, number of steps required for one millimetre is calculated as follows:

$$E_{steps/mm} = \frac{200 \times 16}{40} = 80 \ (steps/mm)$$

## 4.2 **Implementation of Y-axis**

The Y-axis motion is achieved by moving the build platform back and forth on a pair of smooth rods, as shown in Figure 21. A pair of end plates connects each rod of the Y-axis. The two end plates were machined from a plate of iron and were drilled together to ensure that support holes for rods would be parallel. Both end plates of the Y-axis are bolted to aluminium extrusions to form the structural frame of the machine. As aluminium extrusions are available in a huge array of size and length, this feature allows the travel distance of Y-axis can be extended for future upgrades, since the length of aluminium extrusions define the travel capacity of the Y-axis.

As on the X-axis, the carriage on Y-axis features GT2-2mm pitch timing belt with 20 teeth pulley. Hence, the parameter "steps/mm" for calculating the number of steps required to move the respective build platform one millimetre can be reused:

$$E_{steps/mm} = \frac{200 \times 16}{40} = 80 \ (steps/mm)$$

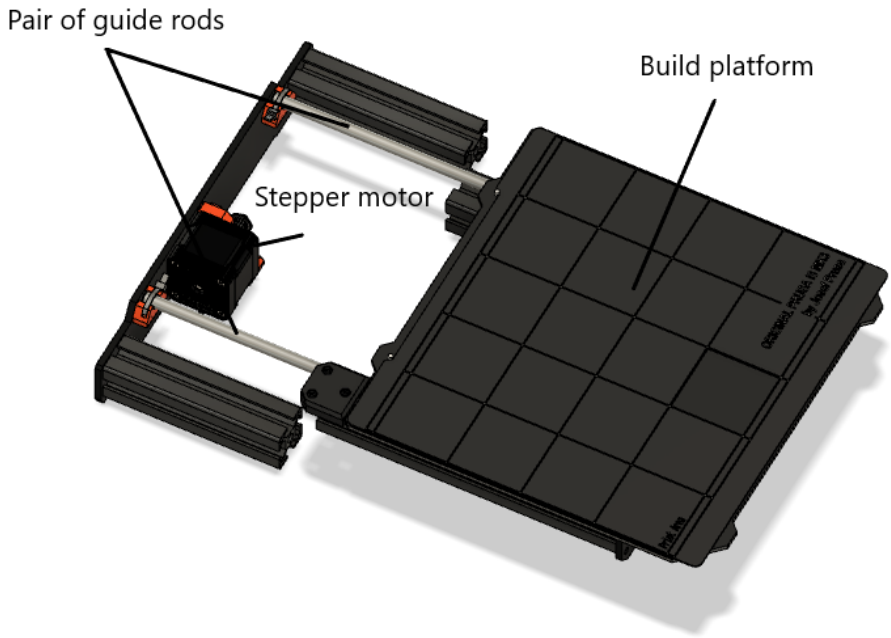


Figure 21. Design of Y-axis (Swesen, 2018)

## 4.3 **Implementation of Z-axis**

On the contrary to the X- and Y-axes, the load on Z-axis is the entire X-axis and the print head assembly, and it moves in small incremental steps as each new layer is printed. The requisite motion for this axis is slow but with great precision. If the Z-axis does not travel the equal amount from layer to layer, the printed object will be distorted dramatically. One straightforward method to improve the precision of Z-axis movement is to increase the motor revolution to linear travel ratio, expressed as "steps/mm", and the stiffness of the drive system. For these reasons, the Z-axis features a drive system using lead screws, as a lead screw drive system offer exactly the combination of features required for this task. First, lead screw drives are non-backdrivable, meaning that the drive motor will not have to exert a huge holding torque to maintain the vertical position of the X-axis and the print head against gravity (Lan, 2013). Secondly, the high force density of lead screw allows a low-torque actuator such as stepper motor to be able to support the weight of the X-axis and the print head. The biggest disadvantage of a lead screw driven system, the slow travel speed, is probably not an issue in this application since the print head is not required to lift frequently.

When using a screw drive system, there are certain attributes to be considered:

- The diameter of the shaft, measured in inches or mm.
- The distance between adjacent threads, called "Pitch".
- The number of "Starts".

– The axial distance the nut moves in one revolution of the screw, called “Lead”. The Lead is equal to the Pitch multiplies the number of Starts.

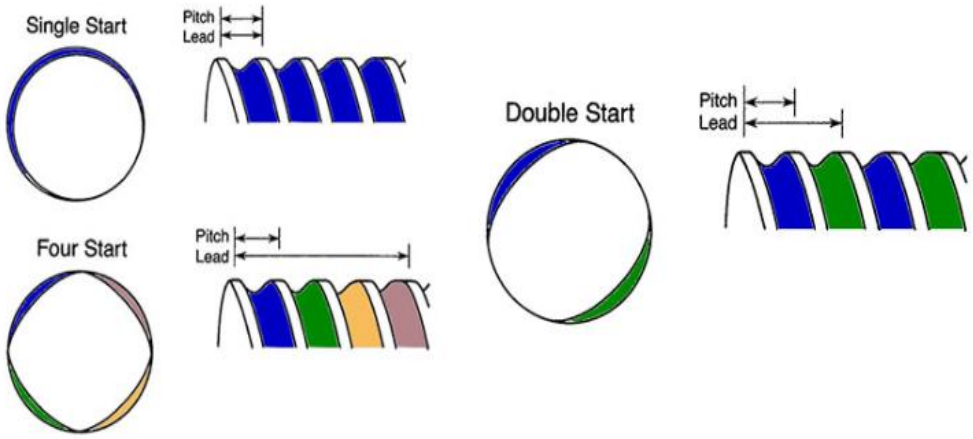


Figure 22. Lead screw’s relation (THOMSON Linear Motion, n.d.)

As a rule of thumb, the larger number of starts, the faster the nut travels. As the Z-axis must carry the combination mass of the X-axis and the print head assembly, two independent lead screws are used to control the Z-axis and provide more support, as shown in Figure 23.

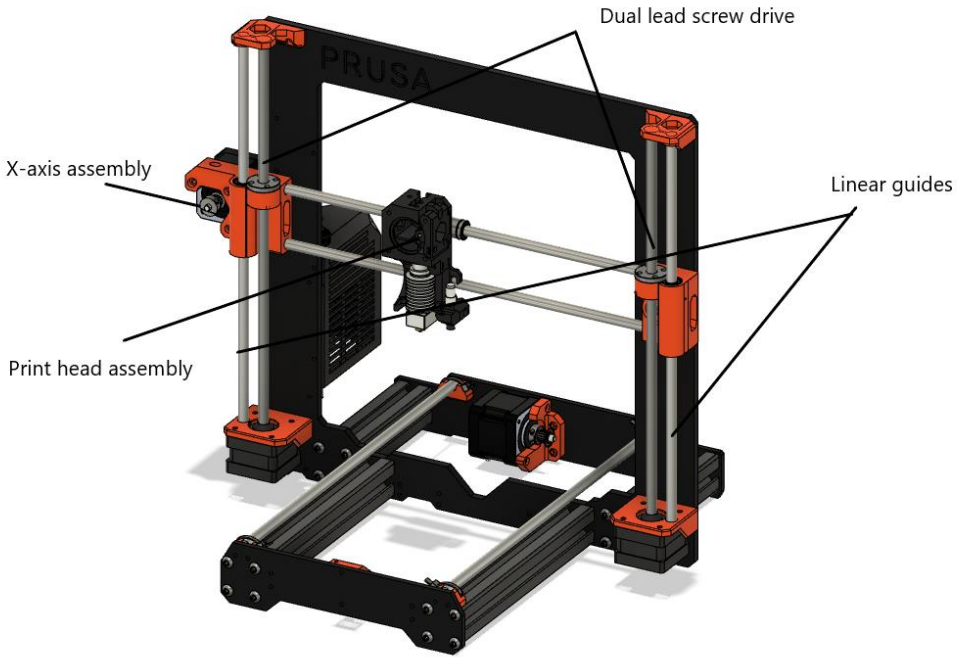


Figure 23. Design of for Z-axis (Swesen, 2018).

Each lead screw drive comprises a stepper motor at its bottom end and a brass nut as a precision unit. Brass nut has a unique bearing property – it is self-lubricating, meaning that as long as the lead screw does not have rust or corrosion, a brass nut will run smoothly for a long term (Rosenberge, 2018). Each brass nut is attached to each end of the X-axis, causing the X-axis and the print head to move up and down when the stepper motor rotates. Each lead screw used for this project is an 300mm length shaft with 2mm Pitch and four starts. Hence, the lead screw has a Lead of 8mm, meaning that each complete revolution of the lead screw or the stepper motor will cause the print head to traverse linearly 8mm. Once having the motor revolution to linear travel ratio, the parameter $E_{steps/mm}$ for calculating the number of steps required to move the respective print head one millimetre can be obtained as follows:

$$E_{steps/mm} = \frac{200 \times 16}{8} = 400\ (steps/mm)$$

## 4.4 **Implementation of extrusion system**

As stated earlier, the extrusion system is responsible for delivering, melting and depositing plastic material onto the build platform. In this project, the extrusion system consists of a single print head attached to the moving carriage, and two extruder drives attached to the static frame of the printer. By providing multiple materials to the print head from stationary extruders, this system separates the complexity of developing a multi-material print head system from a positioning system.

The extruder axis movement is treated in the similar way as X-, Y-, and Z-axes, it must convert the rotary motion of the motor to linear travel of the filament, and move in linear proportion to all other motors, maintaining exactly the same acceleration profile as well as start/stop points. To achieve this goal, each extruder drive comprises a stepper motor and a feeding gear that acts as precision unit to push the filament forward, as seen in Figure 24. In this arrangement, when the drive wheel rotates clockwise as shown, the material filament is driven forward to the print head. Conversely, when it turns the opposite direction, counter-clockwise, the material filament is withdrawn or retracted.

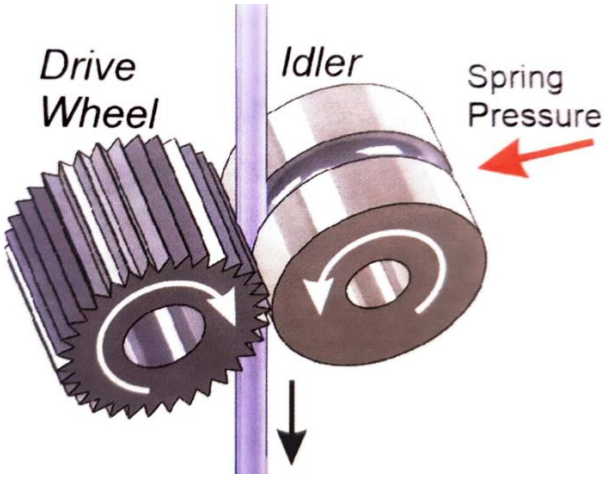


Figure 24. Filament-drive working principle (Rosenberge, 2018).

To enable multi-material printing feature, two extruder drives are used to route different materials to the print head. Before entering the print head, the materials are parked inside the "Y-shaped combiner", as shown in Figure 25. The Y-shaped combiner can accommodate more than one material inside, but only allows one material to get through and into the print head at a time. During the printing job, when the control scheme asks for switching material, the current printing material is retracted back to the Y-shaped combiner far enough so that the other material can take the same route and reach the print head.

Figure 25. Y-shaped combiner

The print head is a purchased item from E3D-Online, one of the leading manufactures for 3D printer components (Petch, 2018). There are two main regions in the structure of the print head, hot end and cold end, as shown in Figure 26. The cold end is clamped to the moving carriage and travels in the printing volume. It is important to prevent this upper part from warming up so much that the carriage and the material are deformed/melted by thermal effect. To eliminate this possibility, the cold end incorporates an active cooling fan which blows room air across a passive Heat Sink. The hot end is a heated chamber into which a Heater Cartridge, a Thermistor and a Nozzle are mounted. The Heater Cartridge supplies heat for melting the plastic material via a large electric current, ensuring mechanical stability and uniform heat transfer. The Thermistor is temperature sensor, particularly an electrical resistor, whose resistance is about 100k Ohm at room temperature. Finally, the Nozzle is the where molten material comes out of the hot end, forming part of the printed object. It is imperative to consider the size of the nozzle, particularly the size of the hole at the end of the hot end, as it defines the resolution of print quality. As a rule of thumb, the smaller the hole, the thinner the printed part. Therefore, small nozzles allow the printer to produce 3D objects with intricate details. Alternatively, a wider nozzle size allows a faster printing production with a minimum level of detail (Rosenberge, 2018).

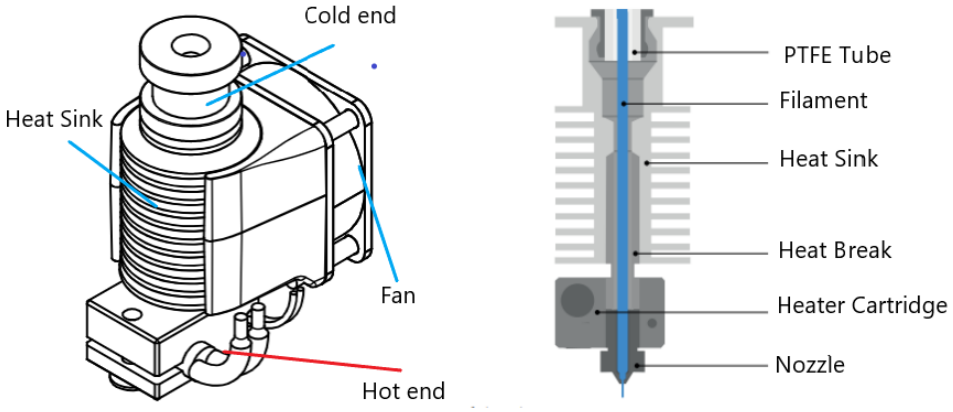


Figure 26. Extrusion structure (V6 Drawings, 2019 )

## 4.5 **Structure frame**

As the rigidity and alignment accuracy of the structural frame is a major concern, the structural frame is machined totally from metal materials, stainless steel and aluminium, as seen in Figure 27. The bottom of the structure uses four T-slot aluminium extrusions for supporting the build platform with the requisite strength. Because the T-slot aluminium are readily tapped with M5 screws at the centre hole, they are bolted directly the vertical frame at 90-degree corner without using complex corner connections. To stiffen the positions of aluminium extrusions, the rear end

and front end are firmly fastened with two stainless steel plates. As a result, the given structural frame delivered required stability and rigidity with a minimal physical footprint. The final construction of the printer can be seen in Figure 28.

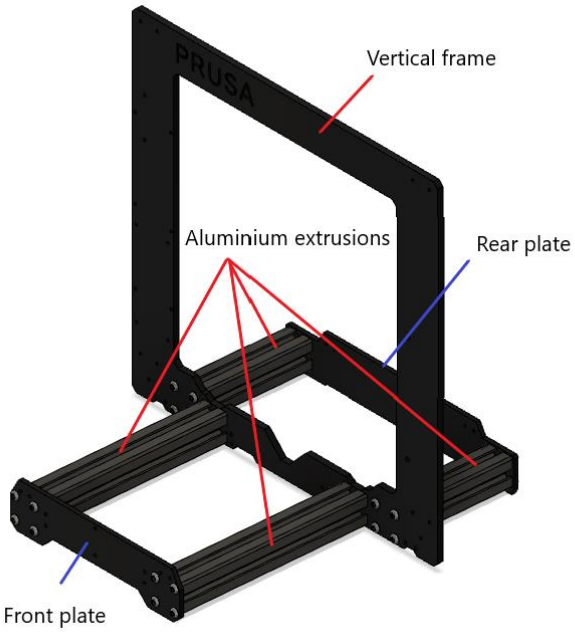


Figure 27. Design of structural frame (Swesen, 2018)

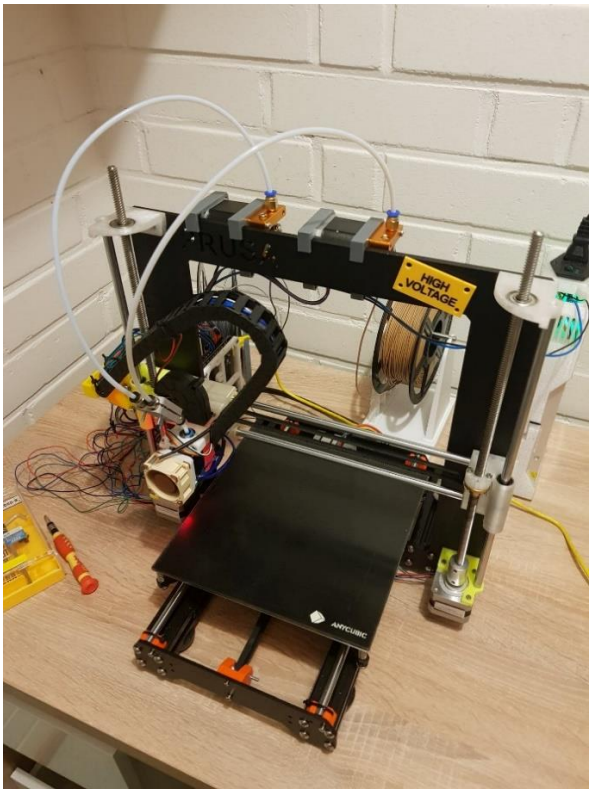


Figure 28. Final construction of the printer

# 5 ELECTRONIC IMPLEMENTATION

## 5.1 Controller

The controller, or the motherboard, is the brain of the electronic system, which uses a programmable memory for performing all the functions that a printer needs to operate. Typically, a controller in the 3D printer consists of a central processor, and lots of input/output (I/O) for interfacing with other devices, namely microstepping drivers, hot end, heated bed, thermistors, etc. Historically, the development of low-cost 3D printers was spurred by the appearance of the Arduino Mega 2560 processor, an 8-bit board. The Arduino Mega must be equipped with a specific board (or "shield") called "RAMPS" to provide the connectors for I/O, voltage regulators and fuses for the higher power requirements, as shown in Figure 29. Since RAMPS and Arduino are designed to be modular, one nice feature of the RAMPS/Arduino Mega combination is that it allows hot-swap and a quick replacement in case of failure (RepRap, 2012).

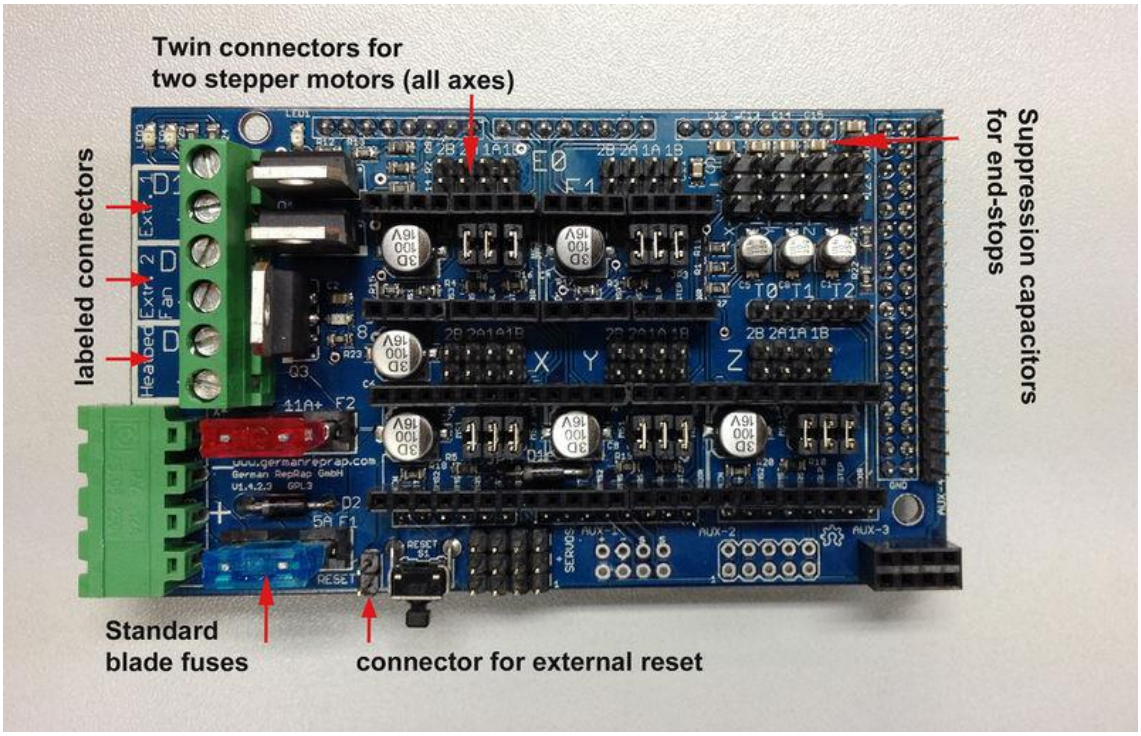


Figure 29. RAMPS board (RepRap, 2012)

Although the RAMPS/Arduino combination was quite powerful in early 3D printers, it recently lost favour to products that is more hardware-wise and combine all the RAMPS/Arduino Mega features on to a single board. Unlike the RAMPS/Arduino combination which can only handle 12VDC power supply, most of the newer single-board controllers are capable of dealing with either 12 VDC or 24 VDC power supply. There are several advantages of using 24VDC over the 12 VDC power supply in 3D printers. First, for high power-consuming devices, such as the Heater Cartridge in the hot end or

the heated bed, the current is halved for a same given wattage and the power dissipated is reduced quadratically with current. Secondly, stepper motors also experience better performance when driven with a higher voltage supply, they response faster with speed changes and allow greater torque at high speeds. Furthermore, these more recently non-Arduino boards also come with a 32-bit processor, which will eventually dominate the scene. The 32-bit processor can handle more complex calculations and higher printing speeds than the 8-bit counterpart, while simultaneously supporting networking tasks, such as Wi-Fi and Bluetooth (Rosenberge, 2018). Particularly, for Delta printers which heavily rely on inverse kinematics and floating-point precision to operate correctly, a wider data path offered by these 32-bit processors is the bottleneck to achieve the highest performance. Due to advantages mentioned above, the SKR V1.1 PRO 32-bit controller was chosen for the control task of the printer.

Figure 30 illustrates the connection diagram which was implemented for the printer.

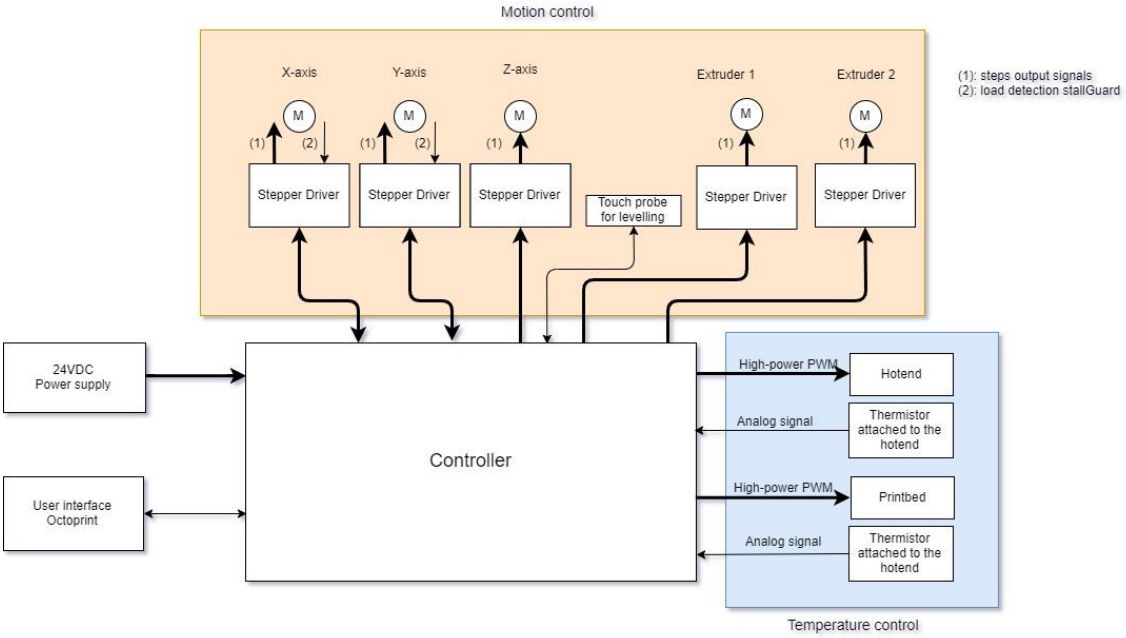


Figure 30. Connection scheme for the printer

## 5.2 **Firmware**

Firmware is the software that runs on the controller and manages all the real-time activities of the printer. That being said, the firmware is responsible for interpreting G-code, turning the motors, coordinating the carriage, controlling temperature, etc. in the printing process. To achieve the intended functionality, Marlin was selected for the firmware of the printer due to its open-source nature and ease of use. The firmware on the printer is the result of work of many people who generously contribute innovative ideas, code improvements and feedback into the public domain. In the Marlin firmware, features are represented as units of

variability and can be configured in the files Configuration.h and Configuration_adv.h. One example feature provided by Marlin is shown Figure 31, where the macro NOZZLE_PARK_FEATURE represents an optional feature. During the build process, the feature will be included in the printer only if the respective macro is enabled.

```
1   #if ENABLED(NOZZLE_PARK_FEATURE)
2   /**
3   * G27: Park the nozzle
4   */
5    inline void gcode_G27() {
6   // Don't allow nozzle parking without homing first
7     if (axis_unhomed_error()) return;
8     Nozzle::park(parser.ushortval('P'));
9    }
10  #endif // NOZZLE_PARK_FEATURE
```

Figure 31. Pre-process code example in Marlin.cpp (Marlin Firmware, 2011)

In the scope of this thesis work, the act of implementing firmware for the printer was generally turning specific features on, or off, and making changes to default parameters, e.g. machine dimensions, steps/mm of axes, power supply voltage, etc. There are a variety of basic and advanced features, the highlights can be briefly summarized as follows:

- stealthChop: a technique that drives the motors using pulse width modulation (PWM) voltage instead of current. As a result, it guarantees nearly inaudible stepping at low speeds or standstill. Because stepper motors operating at low velocities experience a phenomenon known as magnetostriction, which generates audible high-pitch noise.
- stallGuard: a technique that measures the load applying to the motor. In case the load is excessively high, the printer can react to such an event appropriately. For example, when the printer drives an axis to its physical limit and the feedback provided by the driver can be recognized as an end stop. By that way, the motor driver itself can be used as a limit axis sensor, eliminating the need for reference or extra end switches.
- Closed-loop PID heater control: a technique for controlling the printing temperatures, applying for the hot end and the heated bed.
- Automatic Bed Levelling: a technique that adjusts all movement of the carriage to follow the tilt or contours of the build platform. The feature is achieved by using a probe to take several measurements of the print surface and then compensating all irregularities of the surface to the control scheme.

Figure 32 represents the block diagram of the state machine implemented in the firmware.

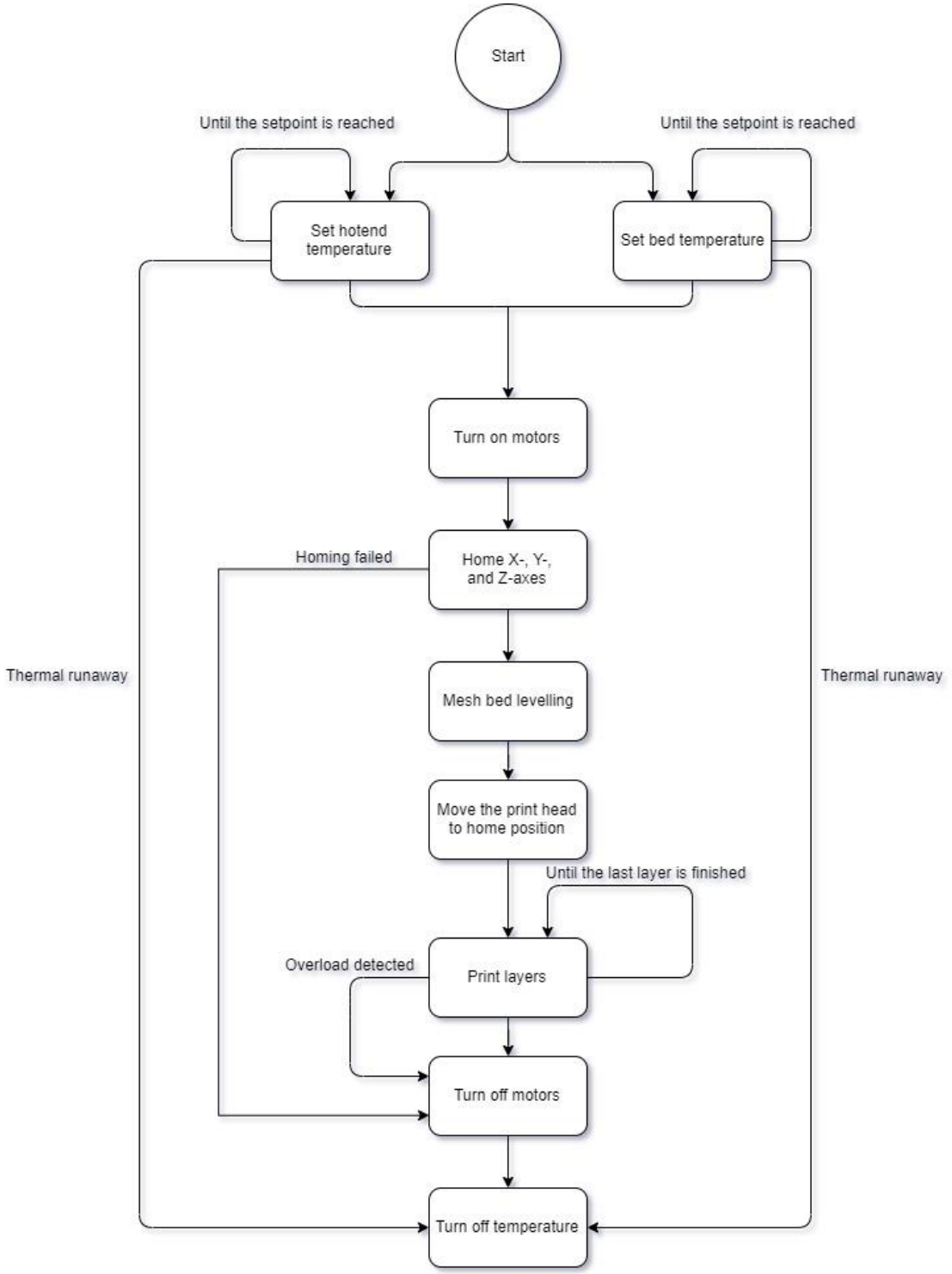


Figure 32. Block diagram of the state machine

## 5.3 **User interface**

As with any appliance or machine, 3D printers require basic means to interact with the user. There is a necessity for reading out the printer's operation mode, current temperatures, printing progress, etc. In addition, the user also needs to transfer data to the printer, such as G-code files, and to issue commands, such as "Start the print", "Stop", "Pause", etc.

Traditionally, most desktop printers resolve this multi-purpose interaction by using LCD display with either rotary push-knob or touch panel, as shown in Figure 33. In order to receive G-code files as input and deliver them to the controller, they are used with a SD Card Reader, making the combination as one of the most popular and economical input/display devices. However, the interface is only available near the actual printer, and the problem grows when the printer is located from a distance in a control room or a workshop, or the user owns a farm of them. Clearly, it is a time-consuming procedure for the user to travel to the control room and repeatedly start the print job for every machine. Due to that fact, it was decided that a wireless connection that allows the user to interact with printers and know their whereabouts is essential.


Figure 33. LCD display (Sercanigk, 2018)

OctoPrint is a well-regarded software solution that lets users communicate with their printer(s) via a web server within Local Area Network (LAN). As a web application, the software is compatible and accessible with most devices and operating systems that have web browsers. Besides, being an open-source platform, OctorPrint offers developers and makers abilities to discuss, share ideas and together contribute to the common goal that is improving the user experience with 3D printers. Thanks to that, the software available tools and plugins are customized for different situations. For example, OctoPrint allows the user to schedule the prints to be started at any time or make triggers if an object from a file is going to be printed partly outside of the printing volume. Due to advantages mentioned above, OctoPrint was selected for user interface of the printer, as shown in Figure 34.

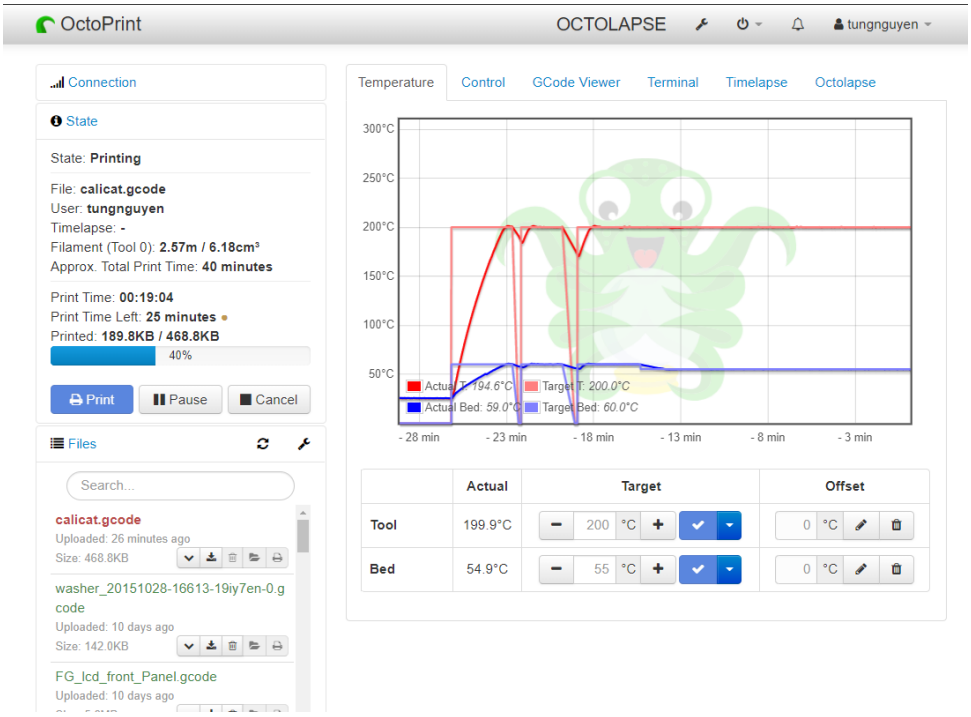


Figure 34. OctoPrint visualization for displaying printing process

# 6 SAMPLE OUTPUTS AND ANALYSIS

The analysis of the printer consisted of two aspects: verification of the structural build and verification of the motion system. Regarding the former aspect, one analytical benefit of 3D printing is that each part is a direct consequence of how well the molten plastic is deposited. For example, if the structural frame is unstable or out-of-square, each time the print head or the build platform moves/accelerates there will be deflections the linear rails. This weakness of the frame will introduce visible permanent distortions in the printed part, the greater the deflection the worse the printed part will be. A common practice to exhibit the possible result of machine instability is printing the XYZ Calibration Cube, as shown in Figure 35.

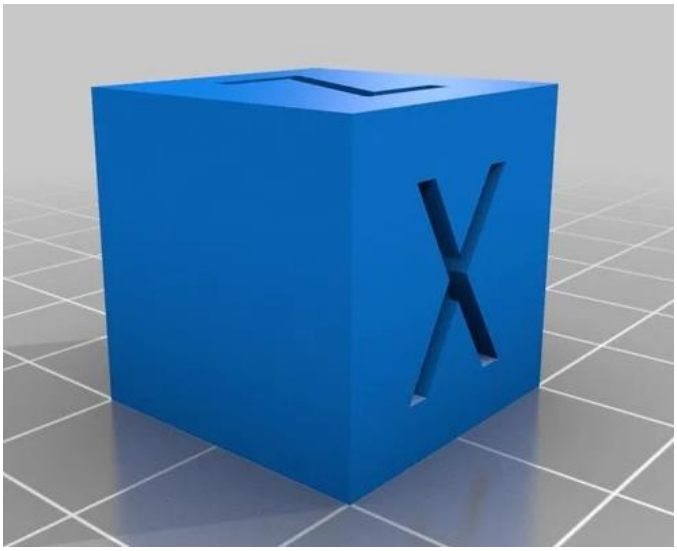

Figure 35. XYZ Calibration Cube (with 20 mm sides) (Thingiverse, 2016)

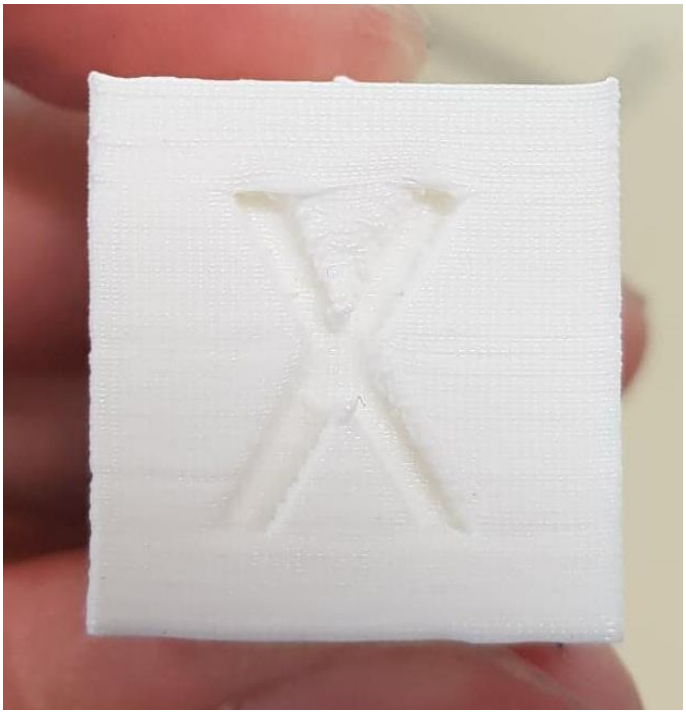

Figure 36. First sample output of calibration cube

In Figure 36, the sample cube printed revealed that vibrations occurred frequently when printing corner features, where a mass experiences sudden changes in velocity. The result of these inconsistencies was first assumed as deformation of critical components, such as frame members, belts and linear rails by the author. Therefore, the first step taken to minimize the effect of vibration was to tighten clearances in mechanical parts and increase the stiffness of the belts. Taking the next step, the values for speed, acceleration and junction deviation in the motion profile were lowered to reduce the impact of sharp transitions. Once the

operating speeds are kept low enough, it will ensure that that any inaccuracies will be strictly mechanical and not caused by the positioning system. Fortunately, these motion settings can be altered readily with the software slicer, instead of re-compiling them for each time printing in the firmware. After a number of trial-and-error cycles of fine tuning, the print quality was improved remarkably. As shown in Figure 37, the printed object measures exactly 20 mm in each side as designed, with Vernier caliper, whose reading error is 0.02 mm.

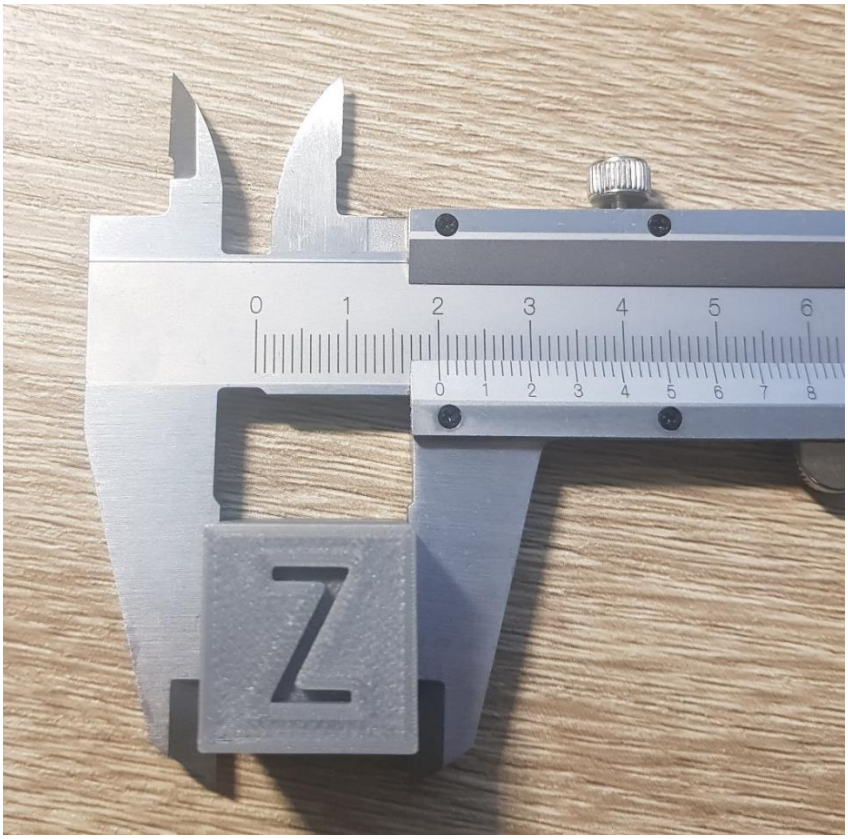


Figure 37. Improved print quality after stiffening mechanical frame

In addition, by comparing key dimensions of the object as designed and as printed, this particular print also provides option for verifying how accurate the positioning system is. The problem is that since the acceleration and operating speeds were reduced from ealier steps, the performance of the motion system could be accurrate as expectation; however, the printing time were also longer than necessary. The empirical target of using 3D printers is to maximize the throughput whilst retaining the highest possible print quality. Therefore, once the structural frame and the belts were verified to be rigid enough to resist various vibrations, the next step is to determine and optimize the capacity of the printer through different motion profiles. On average, it was found that printing object at 120 mm/sec delivered a good balance between speed and quality, as depicted in Figure 38.

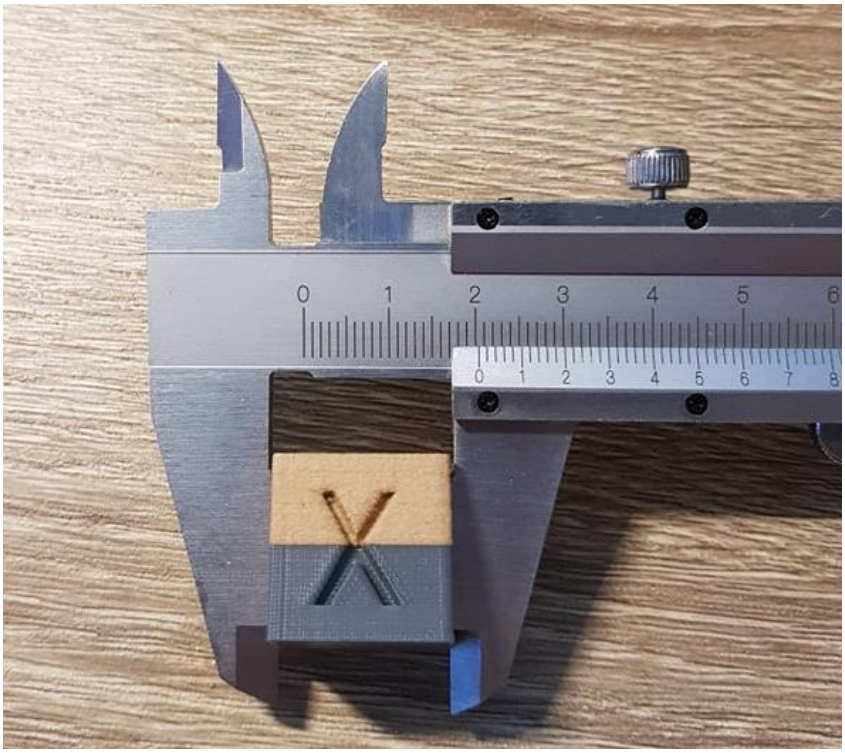

Figure 38. Print quality at 120 mm/sec printing speed

# 7 CONCLUSION

This thesis presents a framework for building a cost-effective 3D printer using stepper motors and other low-level resources. Inexpensive components were utilised where possible, reducing the complexity of the system without sacrificing performance. Based on the information provided here, students or hobbyists can study and replicate the machine with ease for their purposes.

There are possible improvements that could have been implemented in the project. Firstly, the positioning system was operated in a non-feedback fashion, in which the output and the actual position of the carriage being moved have no impact on the control action of the input signals. To address said issue, an appropriate closed-loop controller is to be considered for the future work. Secondly, the multi-material printing capabilities were limited up to two materials, which was not efficient and flexible enough for aesthetics requiring applications. Hence, an automatic switching material mechanism is suggested to replace the current “Y-shaped combiner” design. The alternative switching mechanism could employ a Direct Drive extruder on the print head and a motorized selector head on the static frame. The selector head may have built-in switching gears and a blade, that will cut the filament tips and allow another filament to come in the hot end. In addition, mechanical load tests for printed objects were not conducted in the project due to the lack of time and

instrumentation, and maximum print parts were inherently limited by the chosen design at 200 x 200 x 200 mm.

In conclusion, the empirical targets of fabricating a 3D printer with multi-material upgrade were achieved. The printer was compatible with most types of filament, e.g. PLA, ABS and PETG, and ready to serve continuously 24/7. Besides, the machine produces little to no audible noise during the printing operation, which is approximately 44 dB, often regarded as noise level for a public library. The above-mentioned characteristic allows the printer to be placed and used in public spaces, such as libraries, classrooms, laboratories, offices, etc.

## REFERENCES

3D Printer Power. (2018). Retrieved from 3dprinterpower.com

Bandyopadhyay, A. (2019). *Additive Manufacturing, Second Edition: Edition 2.*

Collins, D. (2017, November 21). *Linear Motion Tips*. Retrieved from What is microstepping?: https://www.linearmotiontips.com/microstepping-basics/

Collins, D. (2018). *What benefits do dovetail slides offer versus other linear bearing types?* Retrieved from Linear Motion Tips: https://www.linearmotiontips.com/what-benefits-do-dovetail-slides-offer-versus-other-linear-bearing-types/

*CoreXY theory.* (2012, April). Retrieved from corexy: http://www.corexy.com/theory.html

*Delta geometry*. (2016, January). Retrieved from RepRap: https://reprap.org/wiki/Delta_geometry

Dolezal, J. (n.d.). *Prusa Research*. Retrieved from https://manual.prusa3d.com/Guide/3.+X-axis+assembly/508

*drylin® linear guides*. (2019). Retrieved from igus: https://www.igus.fi/drylin/linear-guide

Fabian. (2019, July). *How Direct Metal Laser Sintering (DMLS) Really Works*. Retrieved from https://i.materialise.com/blog/en/direct-metal-laser-sintering-dmls/

Franky. (2014, December). *3D Printing Technologies: Stereolithography*. Retrieved from https://i.materialise.com/blog/en/an-intro-to-our-3d-printing-technologies-stereolithography/

Graves, S. (2015, January). *Linear Delta Printer Kinematics.* Retrieved from RepRap: https://reprap.org/wiki/Linear_Delta_Printer_Kinematics

Lan, J. (2013). *Design and Fabrication of a Modular Multi-Material 3D Printer.* Massachusetts: Massachusetts Institute of Technology.

Landry, T. (2016). *Extruders 101: A crash course on an essential component of your 3D printer*. Retrieved from https://www.matterhackers.com/articles/extruders-101:-a-crash-course-on-an-essential-component-of-your-3d-printer

Lopes, L., Silva, A., & Carneiro, O. (2018). Multi-Material 3D Printing: the Relevance of Materials Affinity on the Boundary Interface Performace. *Additive Manufacturing.*

Marlin Firmware. (2011, August). Retrieved from Marlin Firmware

mmar896. (2016, August 1). *4ME3D Mini 3D Printer Design and Creation*. Retrieved from RepRap: https://reprap.org/wiki/4ME3D_Mini

Petch, M. (2018). *2018 3D PRINTING INDUSTRY AWARDS WINNERS ANNOUNCED*. Retrieved from 3D Printing Industry: https://3dprintingindustry.com/news/2018-3d-printing-industry-awards-winners-announced-133578/

Redwood, B. (2017). *The 3D Printing HandBook.* 3D Hubs.

Reeves, P., & Mendis, D. (2015). The Current Status and Impact of 3D Printing Within the Industrial Sector: An Analysis of Six Case Studies. Intellectual Property Office.

RepRap. (2010, April). *Frame material*. Retrieved from RepRap: https://reprap.org/wiki/Frame_material

RepRap. (2012, March). *RAMPS 1.4*. Retrieved from RepRap: https://reprap.org/wiki/RAMPS_1.4

RepRap. (2014, April). *Mechanical arrangement*. Retrieved from RepRap: https://reprap.org/wiki/Mechanical_arrangement

RepRap. (2015, February). *CoreXY*. Retrieved from https://reprap.org/wiki/CoreXY

RepRap. (2016, January). *RepRap*. Retrieved from https://reprap.org/wiki/RepRap

Rosenberge, N. (2018). *Designing 3d printers: Essential Knowledge.*

Santons, R., James, J., Chris, M., & Maalouf, P. (2015). *Deltronic Solutions 3D Printer.* California: Carlifonia Polytechnic State University. Retrieved from Deltronic Delta 3D Printer: https://digitalcommons.calpoly.edu/mesp/278/

Sercanigk. (2018, December). *RepRap Full Graphic Smart Controller LCD*. Retrieved from Thingiverse: https://www.thingiverse.com/thing:3302757

Swesen. (2018). *Original Prusa i3 MK3 for Fusion 360(and STL)*. Retrieved from Thingiverse: https://www.thingiverse.com/thing:3114931

*Thingiverse*. (2016). Retrieved from XYZ 20mm Calibration Cube: https://www.thingiverse.com/thing:1278865

*THOMSON Linear Motion*. (n.d.). Retrieved 2019, from What is the difference between screw pitch and lead?: https://www.thomsonlinear.com/en/support/tips/difference-between-screw-pitch-and-lead

Toglefritz. (2015, July). *3D Printer Linear Motion Systems*. Retrieved from https://toglefritz.com/3d-printer-linear-motion-systems/

TRINAMIC. (2016, November). *StallGuard™*. Retrieved from TRINAMIC: https://www.trinamic.com/technology/adv-technologies/stallguard/

*V6 Drawings*. (2019 ). Retrieved from E3D-Online: https://e3d-online.dozuki.com/c/V6_Drawings

Varotsis, B. A. (2019). *Introduction to FDM 3D printing*. Retrieved from 3dhubs: https://www.3dhubs.com/knowledge-base/introduction-fdm-3d-printing

Zhang, J., Patil, H., Feng, X., & Tiwari, R. (2016). Coupling 3D Printing with Hot-Melt Extrusion to Produce Controlled-Release Tablets. *International Journal of Pharmaceutics* .

Appendix 1

Bill of materials

This appendix lists the commercial off-the-shelf components used in the fabrication of the printer. The estimation of total price is 600€.

Frame

| **Reference #** | **Part name** | **Source** | **Quantity** | **Price/unit (€)** |
|---|---|---|---|---|
| - | T-slotted aluminium extrusion, 205mm long, 4.2mm tapped holes | HAMK Lab | 2 | 8 |
| - | T-slotted aluminium extrusion, 120mm long, 4.2mm tapped holes | HAMK Lab | 2 | 8 |
| 4903M40AH | Rubber feet, packs of 4 | Amazon.de | 4 | 3 |
| B07YTXWXWQ | Aluminium alloy frame | Amazon.de | 1 | 65 |
| | Stainless steel front plate | | | |
| | Stainless steel rear plate | | | |
| | Aluminium alloy Y carriage | | | |

Build platform

| **Reference #** | **Part name** | **Source** | **Quantity** | **Price/unit (€)** |
|---|---|---|---|---|
| AB-ZHM010 | Heated bed, 220 x 220mm | Anycubic | 1 | 24 |
| YPN0147-EU | Compression springs for bed levelling, 20mm long, 7.6mm OD, packs of 4 | Amazon.de | 1 | 6.49 |
| BIQU-3D0403 | BLtouch levelling sensor | BIQU | 1 | 45 |

X-axis and Y-axis

| **Reference #** | **Part name** | **Source** | **Quantity** | **Price/unit (€)** |
|---|---|---|---|---|
| 0778601687288 | TMC5160 v1.2 microstepping driver | KINGPRINT | 2 | 16.75 |
| TB42HT48-1684AC | NEMA 17 single shaft stepper motor | Thingibox | 2 | 12.35 |
| 0700401394035 | Hardened chrome shaft, 10mm diameter, 400mm long | Amazon.de | 4 | 11 |
| 0611702546309 | GT2 timing belt with pulley | Amazon.de | 1 | 11.7 |
| 4260537859038 | LM8UU DryLin® bearing, 15mm OD, 24mm long, packs of 12 | igus Inc. | 1 | 12 |

Appendix 2

Bill of materials

Z-axis

| Reference # | Part name | Source | Quantity | Price/unit (€) |
|---|---|---|---|---|
| 0778601687288 | TMC5160 v1.2 microstepping driver | KINGPRINT | 1 | 16.74 |
| TB42HT48-1684AC | NEMA 17 stepper motor, single shaft, 4.40Kg.cm | Thingibox | 2 | 12.34 |
| 0700401394035 | Hardened chrome shaft, 10mm diameter, 400mm long | Amazon.de | 2 | 11 |
| ZM3D-SGT8300 | Stainless steel lead screw, 300mm long, 4 start, 2mm pitch, packs of 2 | Amazon.de | 1 | 18 |
| 0794419254689 | Roller bearing, 28mm OD, packs of 10 | Amazon.de | 1 | 10.5 |
| 0756832362129 | Shaft coupler, 5-8mm diameter, packs of 2 | 3D FREUNDE | 1 | 10 |

Extruder and print head

| Reference # | Part name | Source | Quantity | Price/unit (€) |
|---|---|---|---|---|
| 43212100 | V6 all-metal hotend, Bowden style, 24 V | E3D | 1 | 61 |
| LK02-UK | A4988 microstepping driver, packs of 5 | Longruner | 1 | 11 |
| TB42HT48-1684AC | NEMA 17 stepper motor, single shaft, 4.40Kg.cm | Thingibox | 2 | 12.34 |
| 0605175674188 | PTFE tube, 100mm long | Amazon.de | 1 | 18 |

Controller and power supply

| Reference # | Part name | Source | Quantity | Price/unit (€) |
|---|---|---|---|---|
| 0778601687479 | SKR v1.3, 32-bit controller | KINGPRINT | 1 | 45 |
| 2111MO6S003F | Coupler socket plug with fuse | Hifi Lab | 1 | 6.7 |
| LRS-350-24 | AC/DC power supply, 24V-350W | Meanwell | 1 | 34 |

Appendix 3

The CAD drawing of rear and front plate

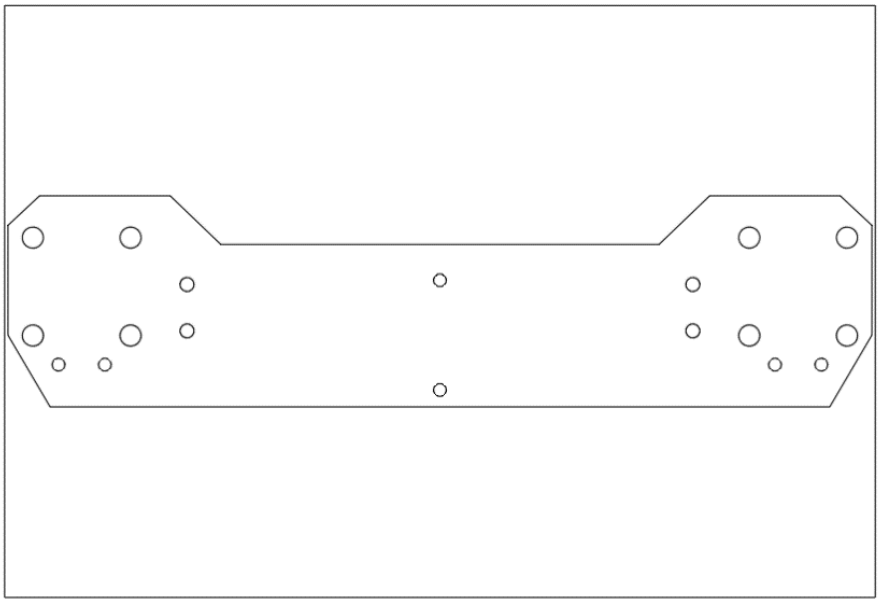

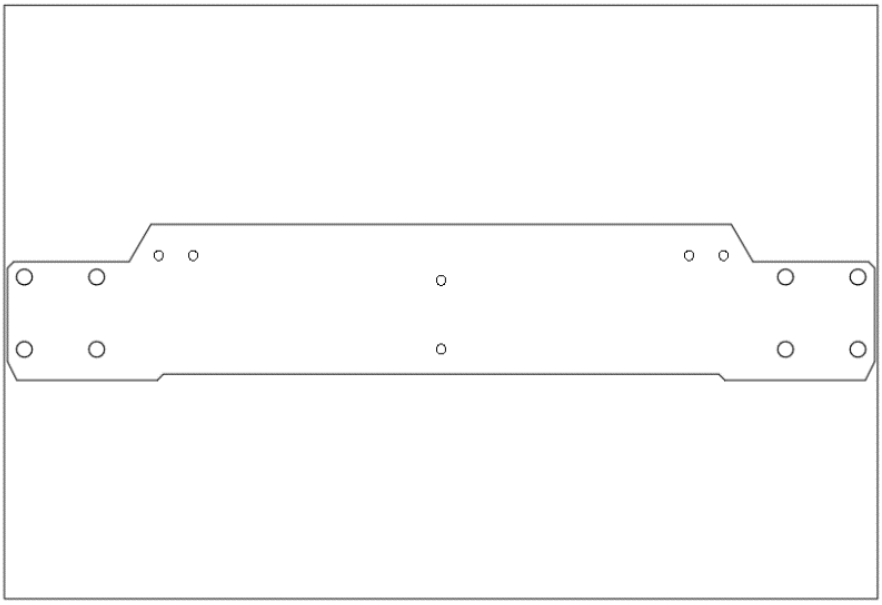

Appendix 4

The CAD drawing of frame and Y carriage